

AD-A221 708

4

AD

AD-E402 034

Contractor Report ARFSD-CR-90005

**DESIGN OF ROBUST CONTROLLERS FOR TURRET-GUN SYSTEM  
USING REDUCED ORDER MODELS**

Vittal S. Rao  
602 Fox Creek Road  
Rolla, MO 65401

Michael Mattice  
Project Engineer  
ARDEC

April 1990



US ARMY  
ARMAMENT MUNITIONS  
& CHEMICAL COMMAND  
ARMAMENT RDE CENTER

**U.S. ARMY ARMAMENT RESEARCH, DEVELOPMENT AND  
ENGINEERING CENTER**

**Fire Support Armaments Center**

**Picatinny Arsenal, New Jersey**

Approved for public release; distribution unlimited.

The views, opinions, and/or findings contained in this report are those of the author(s) and should not be construed as an official Department of the Army position, policy, or decision, unless so designated by other documentation.

The citation in this report of the names of commercial firms or commercially available products or services does not constitute official endorsement by or approval of the U.S. Government.

Destroy this report when no longer needed by any method that will prevent disclosure of contents or reconstruction of the document. Do not return to the originator.

UNCLASSIFIED  
SECURITY CLASSIFICATION OF THIS PAGE

## REPORT DOCUMENTATION PAGE

1a. REPORT SECURITY CLASSIFICATION UNCLASSIFIED			1b. RESTRICTIVE MARKINGS		
2a. SECURITY CLASSIFICATION AUTHORITY			3. DISTRIBUTION/AVAILABILITY OF REPORT  Approved for public release; distribution is unlimited.		
2b. DECLASSIFICATION/DOWNGRADING SCHEDULE					
4. PERFORMING ORGANIZATION REPORT NUMBER			5. MONITORING ORGANIZATION REPORT NUMBER Contractor Report ARFSD-CR-90005		
6a. NAME OF PERFORMING ORGANIZATION Vittal S. Rao		6b. OFFICE SYMBOL	7a. NAME OF MONITORING ORGANIZATION ARDEC, FSAC		
6c. ADDRESS (CITY, STATE, AND ZIP CODE) 602 Fox Creek Road Rolla, MO 65401			7b. ADDRESS (CITY, STATE, AND ZIP CODE) Fire Control Division (SMCAR-FSF-RC) Picatinny Arsenal, NJ 07806-5000 (cont)		
8a. NAME OF FUNDING/SPONSORING ORGANIZATION ARDEC, IMD STINFO Br		8b. OFFICE SYMBOL SMCAR-IMI-I	9. PROCUREMENT INSTRUMENT IDENTIFICATION NUMBER DAAL03-86-D-0001		
8c. ADDRESS (CITY, STATE, AND ZIP CODE) Picatinny Arsenal, NJ 07806-5000			10. SOURCE OF FUNDING NUMBERS		
			PROGRAM ELEMENT NO.	PROJECT NO.	TASK NO. WORK UNIT ACCESSION NO.
11. TITLE (INCLUDE SECURITY CLASSIFICATION)  DESIGN OF ROBUST CONTROLLERS FOR TURRET-GUN SYSTEM USING REDUCED ORDER MODELS					
12. PERSONAL AUTHOR(S) Vittal S. Rao, Rolla, MO and Michael Mattice, ARDEC, Project Engineer					
13a. TYPE OF REPORT Final		13b. TIME COVERED FROM Dec 88 TO Nov 89		14. DATE OF REPORT (YEAR, MONTH, DAY) April 1990	
15. PAGE COUNT 67					
16. SUPPLEMENTARY NOTATION Task was performed under a Scientific Services Agreement issued by Battelle, Research Triangle Park Office, 200 Park Drive, P. O. Box 12297, Research Triangle Park, NJ 27709.					
17. COSATI CODES			18. SUBJECT TERMS (CONTINUE ON REVERSE IF NECESSARY AND IDENTIFY BY BLOCK NUMBER)		
FIELD	GROUP	SUB-GROUP	Robust controllers Reduced order models Frequency weighted LQG controllers		
19. ABSTRACT (CONTINUE ON REVERSE IF NECESSARY AND IDENTIFY BY BLOCK NUMBER)  Reduced order modeling techniques are used to design lower order robust controllers for a turret-gun system. The balance truncation, Routh approximation, Litz's modal techniques are used to derive reduced order models. A critical comparison to time and frequency response characteristics between original and reduced order models is made. The linear quadratic Gaussian with loop transfer recovery (LQG/LTR) methodology is employed to design robust controllers using reduced order models. The spillover problem associated with a reduced order model design procedure is also investigated. The frequency shaped linear quadratic regulator (FSLQR) with output feedback design methodology is also presented in this report.					
20. DISTRIBUTION/AVAILABILITY OF ABSTRACT <input type="checkbox"/> UNCLASSIFIED/UNLIMITED <input checked="" type="checkbox"/> SAME AS RPT. <input type="checkbox"/> DTIC USERS			21. ABSTRACT SECURITY CLASSIFICATION UNCLASSIFIED		
22a. NAME OF RESPONSIBLE INDIVIDUAL I. HAZNEDARI			22b. TELEPHONE (INCLUDE AREA CODE) (201) 724-3316		22c. OFFICE SYMBOL SMCAR-IMI-I

DD FORM 1473, 84 MAR

UNCLASSIFIED  
SECURITY CLASSIFICATION OF THIS PAGE

7a. and 7 b. Name and Address of Monitoring Organization: (cont)

ARDEC, FSAC

P.O. Box 12211

Research Triangle Park, NC 27709-2211

## ACKNOWLEDGEMENTS

I wish to thank the U.S. Army Research Office and Army Armament Research Development and Engineering Center for Sponsorship of this research. The application of robust controller design methodology to a turret-gun system mounted on helicopters is an interesting and challenging problem. Dr. Norman P. Coleman Jr. suggested this problem and provided constant encouragement and an excellent atmosphere for conducting research.

The author also wishes to thank Mr. Michael S. Mattice for the innumerable hours of fruitful discussions. Mr Mattice always had the time to share his ideas and discuss the development of the project.

Many thanks are due to Ms. Kitty Collins of Battelle for excellent administration of the project.

Accession For		
NTIS GRA&I	<input checked="checked" type="checkbox"/>	
DTIC TAB	<input type="checkbox"/>	
Unannounced	<input type="checkbox"/>	
Justification		
By		
Distribution/		
Availability Codes		
Dist. Statement		
A-1		



## TABLE OF CONTENTS

	Page
I. Introduction.....	1
II. Research Objectives.....	2
III. Description of the Turret-Gun System.....	3
IV. Reduced Order Modeling Techniques.....	3
A. Balanced Realization Method.....	3
B. Routh Approximation Method.....	5
C. Litz's Modal Method.....	8
V. State Variable Model of the Turret-Gun System.....	10
VI. Derivation for Reduced Order Models.....	14
VII. Robust Controllers.....	18
A. Frequency Domain Uncertainties.....	18
B. Time Domain Uncertainties.....	21
C. Robustness.....	21
D. Properties of Feedback System.....	21
E. LQG/LTR Design Methodology.....	25
VIII. Frequency Shaped Linear Quadratic Regulator.....	32
A. Disturbance Attenuation by FSLQR.....	36
B. Robustness Enhancement of FSLQR Method.....	37
IX. FSLQR with Output Feedback Methodology.....	40
A. Performance Robustness Design Guidelines.....	43
B. Loop Shaping Procedures.....	44
X. Design of Reduced Order Robust Controllers.....	46
XI. Conclusions.....	54
References.....	55
Distribution List.....	59

## LIST OF TABLES

		Page
Table I	Eigenvalues, Damping Ratio and Natural Frequencies of Azimuth Axis System.....	13
II	Comparison of Eigenvalues .....	15
III	Frequency-Shaped Weighting Elements for $Q(s)$ .....	45
IV	Frequency-Shaped Weighting Elements for $R(s)$ .....	46
V	Eigenvalues Comparisons of Closed Loop System.....	49
VI	Gain Margin and Phase Margin Comparisons .....	49

## LIST OF FIGURES

		Page
FIG 1.	Schematic Diagram of Azimuth Axis System.....	11
2.	Block Diagram Representation of Azimuth Axis System.....	12
3.	Frequency Response Plots.....	16
4.	Step Response Plots.....	17
5.	Frequency Domain Representations of Model Uncertainty.....	19
6.	Bound on Frequency Domain Multiplicative Uncertainty.....	20
7.	Typical Feedback System.....	22
8.	Block Diagram Representation of FSLQR Closed Loop System..	35
9.	Closed Loop System wiht Disturbances .....	36
10.	Implementation of Full Order Controller .....	47
11.	Implementation of Reduced order Controller.....	47
12.	Singular Value Plots .....	45
13.	Step Response Comparisons.....	51
14.	Ramp Response Comparisons.....	52
15.	Step Response Disturbances.....	53



## I. INTRODUCTION

Improvements in robust performance of a Turret-Gun System mounted on helicopters, can significantly enhance the mission capabilities of light attack helicopters. Designing controllers for a Turret-Gun System, whose mathematical model is subject to uncertainties is an interesting and challenging problem. The uncertainties in the model may arise from unmodeled dynamics, parameter variations, linearization of nonlinear elements, sensor noises etc. A control strategy which can guarantee stability and provide satisfactory performance in the presence of model uncertainties, is called a robust controller. Among the various design methods for robust controllers, the linear quadratic Gaussian with loop transfer recovery (LQG/LTR) design procedure [1] has many advantages. This methodology will result in control systems with excellent stability robustness, command following, disturbance rejection and sensor noise suppression properties.

A frequency-shaped linear quadratic regulator (FSLQR) methodology [2] based on the frequency domain penalties to the state variables and inputs in the cost functional has received considerable attention in the literature [3-6].

The LQG/LTR and FSLQR design methodologies have been employed to design robust controllers for a Turret Gun System.

One of the important problems in the control of a Turret-Gun system is to approximate a high-order, complex mathematical model of the system with a low-order, simpler model. The resulting reduced order models are useful for designing and implementing robust controllers for a Turret-Gun System. This methodology will provide simplicity of implementation and reduction in hardware requirements.

The Turret-Gun System contains nonlinear elements, such as gear trains, servo valves, hydraulic motors etc. In this system, the firing disturbances excite the structural modes. Integrated Systems Inc. (ISI) has developed a detailed nonlinear model and identified various parameters of the model [7]. A linear quadratic Gaussian with loop transfer recovery (LQG/LTR) controller is designed for the gun system using linearized models. We

encountered the convergence/numerical integration problems in the simulation of this controller along with the non-linear plant. It is also noticed that there is a large spread of eigenvalues of the linear model [8]. For the convergence of the control algorithms and their easy implementation, controllers are designed using reduced order models.

A large number of techniques are available in the literature for deriving reduced order models. In this report reduced order models for Turret-Gun Systems are designed using balanced realization [9], Litz's modal technique [10] and Routh Approximation [11,12] methods. A critical comparison of time and frequency response characteristics between an original and reduced order models is made. The choice of a reduced order model is very significant for the validity of reduced order robust controllers. The linear quadratic Gaussian with loop transfer recovery methodology is employed to design reduced order robust controllers. The discarded modes in the original system representation can be excited by a reduced order controller and may destabilize the control system. This problem is known as spillover problem and is eliminated in the proposed design methodology.

## II RESEARCH OBJECTIVES

The research objectives are

- (1) Design an LQG/LTR controller for a Turret-Gun System which has good command following for step, ramp and acceleration inputs.
- (2) Design a frequency shaped linear quadratic regulator (FSLQR) for minimizing high frequency uncertainties.
- (3) Design of LQG/LTR and FSLQR controllers using reduced order models.
- (4) Stability and performance in the presence of uncertainties.
- (5) Simulation studies incorporating reduced order controller with a nonlinear plant.

### III DESCRIPTION OF THE TURRET-GUN SYSTEM

The Turret-Gun System consists of a 30 mm chain gun driven by an electrical motor and is capable of firing 600 rounds per minute. Weapon pointing commands are generated by an integrated helmet and display sight system using a fire control computer.

The gun is mounted within a cradle using a brass slide mechanism which allows for recoil movement. Recoil adapters are mounted between the recoiling mass of the gun and the cradle to absorb some of the recoil force. The cradle and gun assemblies are attached to a fork using two trunnion pins. One trunnion pin has a resolver built into it. This resolver provides the elevation pointing error to the turret control box. The elevation axis positioning is accomplished through the use of a servo valve controlled, double acting hydraulic cylinder. The piston has unequal cross-sectional areas to account for gravitational effects. A delta hydraulic pressure transducer provides rate feedback information to the turret control box.

The fork assembly is held in place by the Azimuth housing. The housing holds a rotary hydraulic motor and a gearbox. The housing also holds a train rate sensor which measures the angular velocity of the Gun/Cradle/Fork unit, and a resolver for measuring the angular position. The Azimuth housing, fork, cradle and gun are attached to the vehicle's hull.

### IV REDUCED - ORDER MODELING TECHNIQUES

In this Section a brief review of various reduced order modeling techniques is given.

#### (A) Balanced Realization Method:

Among the various model reduction techniques, reduced order models derived using the balancing-truncation [9] technique have many advantages. This technique is based on controllability and observability (location of actuators and sensors) considerations of the plant. The subsystem corresponding to dominant (non-dominant) singular values of the balanced

Grammians is termed the strong (weak) subsystem. By approximating the weak subsystem at  $\omega = 0$ , a reduced order model is derived. Let the state variable representation of a Turret-Gun System be given by

$$\dot{x} = Ax + Bu \quad \dots(1)$$

$$y = Cx + Du \quad \dots(2)$$

Let  $x_b = Tx \quad \dots(3)$

where T is a linear transformation matrix which transforms the system representation into balance realization form.

$$\dot{x}_b = A_{bal}x_b + B_{bal}u \quad \dots(4)$$

$$y = C_{bal}x_b + D_{bal}u \quad \dots(5)$$

The Hankel singular values ( $\sigma_i$ ) are determined by

$$\sigma_i = \sqrt{\lambda_i(PQ)} \quad i = 1, 2, \dots, n \quad \dots(6)$$

where P and Q are controllability and observability grammians.

The balanced realization Eqns (4 and 5) are partitioned as

$$\dot{x}_1 = A_{11}x_1 + A_{12}x_2 + B_1u \quad \dots(7)$$

$$\dot{x}_2 = A_{21}x_1 + A_{22}x_2 + B_2u \quad \dots(8)$$

$$y = C_1x_1 + C_2x_2 + Du \quad \dots(9)$$

The approximation employed is

$$X_2(s) \approx -A_{22}^{-1}A_{21}X_1(s) - A_{22}^{-1}B_2U(s) \quad \dots(10)$$

and the reduced order model is given by

$$\dot{x}_r = A_r x_r + B_r u \quad \dots(11)$$

$$y_r = C_r x_r + D_r u \quad \dots(12)$$

where

$$A_r = A_{11} - A_{12} A_{22}^{-1} A_{21} \quad \dots(13)$$

$$B_r = B_1 - A_{12} A_{22}^{-1} B_2 \quad \dots(14)$$

$$C_r = C_1 - C_2 A_{22}^{-1} A_{21} \quad \dots(15)$$

$$D_r = D_1 - C_2 A_{22}^{-1} B_2 \quad \dots(16)$$

The reduced order models possess the following properties [13] which are very useful in the design of reduced order LQG/LTR controllers.

- (i) The reduced order models preserve stability, controllability, observability and minimality.
- (ii) The steady state values of the original system and reduced order model are identical.
- (iii) Error bound of the reduced order model

$$\bar{\sigma} [G(j\omega) - G_r(j\omega)] < 2 \sum_{i=r+1}^n \sigma_i \quad \forall \quad \omega \quad \dots(17)$$

- (iv) Reduced order models have good frequency response match at low frequencies.

#### (B) Routh Approximation Method

The Routh Approximation method proposed by Hutton and Friedland [11]. is based on the Routh Stability criterion. This reduced order methodology has the following properties.

- (i) The reduced order model is guaranteed stable, if the original system is stable.
- (ii) The sequence of Routh approximants converge monotonically to the original system in terms of the impulse response energy.
- (iii) The method does not require any information about the system eigenvalues and eigenvectors.

Rao, et al [12] have developed a Routh canonical realization in time domain for single input - single output systems. This procedure eliminates the reciprocal transformations used in the Hutton and Friedland [11] procedure.

Consider a linear system represented in the phase canonical form

$$\dot{x} = Ax + Bu \quad \dots(18)$$

$$y = Cx \quad \dots(19)$$

where  $x$  is an  $n$ -vector,  $u$  and  $y$  are scalar.

The Routh canonical form is obtained by considering a linear transformation

$$z = Px \quad \dots(20)$$

and is given by

$$\dot{z} = Fz + Gu \quad \dots(21)$$

$$y = Ez \quad \dots(22)$$

$$\text{where } F = PAP^{-1}, \quad G = PB, \quad E = CP^{-1} \quad \dots(23)$$

The system matrices  $F$  and  $G$  can be written as

$$F = \begin{bmatrix} -\gamma_1 & 0 & -\gamma_3 & 0 & -\gamma_5 & \dots & -\gamma_n \\ 0 & 0 & \gamma_3 & 0 & \gamma_5 & \dots & \gamma_n \\ -\gamma_1 & -\gamma_2 & -\gamma_3 & 0 & -\gamma_5 & \dots & -\gamma_n \\ \vdots & & & & & & \\ -\gamma_1 & -\gamma_2 & -\gamma_3 & -\gamma_4 & -\gamma_5 & \dots & -\gamma_n \end{bmatrix}$$

$$G = [1 \ 0 \ 1 \ 0 \ 1 \ \dots \ 1]^T \quad \text{for } n \text{ odd} \quad \dots(24)$$

$$F = \begin{bmatrix} 0 & \gamma_2 & 0 & \gamma_4 & \dots & \gamma_n \\ -\gamma_1 & -\gamma_2 & 0 & -\gamma_4 & \dots & -\gamma_n \\ 0 & 0 & 0 & \gamma_4 & \dots & \gamma_n \\ \vdots & & & & & \\ -\gamma_1 & -\gamma_2 & -\gamma_3 & -\gamma_4 & \dots & -\gamma_n \end{bmatrix}$$

$$G = [0 \ 1 \ 0 \ 1 \ \dots \ 1]^T \quad \text{for } n \text{ even} \quad (25)$$

where the values of  $\gamma_i$  are obtained from a Routh table using the characteristic equation of the transfer function  $C(sI-A)^{-1}B$ .

Let the characteristic equation be

$$f(s) = s^n + a_1 s^{n-1} + a_2 s^{n-2} + \dots + a_n = 0 \quad \dots(26)$$

Then the Routh table can be constructed as

$$\begin{array}{cccccc} a_n & a_{n-2} & a_{n-4} & \dots & a_2 & 1 \\ a_{n-1} & a_{n-3} & a_{n-5} & \dots & a_1 & 0 \\ a_0^2 & a_2^2 & a_4^2 & \dots & & \\ a_0^3 & a_2^3 & \dots & & & \\ \vdots & & & & & \\ a_0^n & & & & & \end{array} \quad \dots(27)$$

The  $\gamma_i$  are given by

$$\gamma_1 = \frac{a_n}{a_{n-1}}, \quad \gamma_2 = \frac{a_{n-1}}{a_0^2}, \quad \gamma_3 = \frac{a_0^2}{a_0^3} \dots \gamma_n = \frac{a_0^{n-1}}{a_0^n}$$

The transformation matrix P can be extracted from the Routh table as

$$P = \begin{bmatrix} a_{n-1} & 0 & a_{n-3} & 0 & \dots & 1 \\ 0 & a_0^2 & 0 & a_2^2 & \dots & 0 \\ 0 & 0 & a_0^3 & 0 & & 1 \\ \vdots & & & & & \\ 0 & 0 & 0 & 0 & \dots & 1 \end{bmatrix} \quad \text{for } n \text{ odd} \quad \dots(28)$$

For an even order  $n$ , the last column of  $P$  is replaced by

$$[0 \ 1 \ 0 \ 1 \ \dots \ 0 \ 1]^T$$

The output matrix  $E$  can be evaluated using the relationship

$$E = CP^{-1} \quad \dots(29)$$

A reduced order model is derived by discarding  $z_{r+1}, \dots, z_n$  and is given by

$$\dot{x}_r = A_r x_r + B_r u \quad \dots(30)$$

$$y_r = C_r x_r \quad \dots(31)$$

where

$$A_r = DFD^T, \quad B_r = DG, \quad C_r = ED^T$$

$$\text{and } D = [I_r \ : \ 0]_{r \times n}$$

### (C) Litz's Modal Method

The reduced order models derived on the basis of modal techniques play a very important role in the design of controllers for large scale systems. A large number of modal techniques are available in the literature [14]. Litz [10] has developed a reduced order model based on a dominance measure and permits larger reductions in size for the same accuracy. A brief review of this method is given below:



Consider a linear system represented by

$$\dot{x} = Ax + Bu \quad \dots(32)$$

Let  $x = Pz \quad \dots(33)$

where P is a transformation matrix which transforms the given system into Jordan canonical form

$$\dot{z} = \Lambda z + Gu \quad \dots(34)$$

A dominance measure is introduced by Litz, to determine dominant modes to be retained, most sensitive state variables and an appropriate order for the reduced model. Equations (33) and (34) are partitioned as shown below:

$$\begin{bmatrix} x_1 \\ x_2 \end{bmatrix} = \begin{bmatrix} p_{11} & p_{12} \\ p_{21} & p_{22} \end{bmatrix} \begin{bmatrix} z_1 \\ z_2 \end{bmatrix} \quad \dots(35)$$

$$\begin{bmatrix} \dot{z}_1 \\ \dot{z}_2 \end{bmatrix} = \begin{bmatrix} \Lambda_1 & 0 \\ 0 & \Lambda_2 \end{bmatrix} \begin{bmatrix} z_1 \\ z_2 \end{bmatrix} + \begin{bmatrix} G_1 \\ G_2 \end{bmatrix} u \quad \dots(36)$$

where  $z_1$  and  $z_2$  represent dominant and nondominant states respectively.

To derive a reduced order model, the following approximation is introduced:

$$\tilde{z}_2 \approx Ez_1 \quad \dots(37)$$

From Equations (35,36 and 37)

$$x_1 = (P_{11} + P_{12}E)z_1 = Fz_1 \quad \dots(38)$$

$$\dot{z}_1 = \Lambda_1 z_1 + G_1 u$$

Let  $x_r = Fz_1 \quad \dots(39)$

where  $F = (P_{11} + P_{12}E)$  is a linear transformation matrix.

The reduced order model is given by

$$\dot{x}_r = A_r x_r + B_r u \quad \dots(40)$$

$$\text{where } A_r = F \Lambda_1 F^{-1} \text{ and } B_r = F G_1 \quad \dots(41)$$

The matrix E is determined optimally through the use of Lagrange multipliers to minimize a weighted integral of the square of the error between  $\tilde{z}_2$  and  $z_2$ . The matrix E is given by

$$E = \Lambda_2^{-1} [S + (G_2 - S T^{-1} G_1)(G_1^* T^{-1} G_1)^{-1} G_1^*] T^{-1} \Lambda_1 \quad \dots(42)$$

where

$$(S)_{i,j} = -\frac{1}{\lambda_{m+i} \bar{\lambda}_j} (G_2 Q G_1^*)_{ij}$$

$$(T)_{i,j} = -\frac{1}{\lambda_{m+i} \bar{\lambda}_j} (G_2 Q G_1^*)_{ij}$$

## V STATE VARIABLE MODEL OF THE TURRET-GUN SYSTEM

A model of the turret-gun system which relates inputs and outputs is needed for control design purposes. A detailed nonlinear model of the system was developed by Integrated Systems Inc. [7]. A separate model for azimuth and elevation axis were developed as the coupling between them is minimal. The azimuth axis system (Fig 1) consists of three physically identifiable sections: (1) servovalve (2) hydraulic motor/gearbox and (3) gun plant. A block diagram representations of this is shown in Fig 2. A linear state variable model of the azimuth axis system is obtained by using system build and analyzing system features of Matrix x. The state variable model derived at the nominal operating point ( $t = 0.04$ ) has 13 eigenvalues values and the damping factors, natural frequencies of this system are given in Table I. The input and output variables are azimuth current and train rate respectively. The mode at -19.385 is not controllable with the selected input, hence a minimal realization of the system is derived by neglecting this mode. The order of the model is 12 and it is noticed that there is a large spread in the eigenvalues of this model.

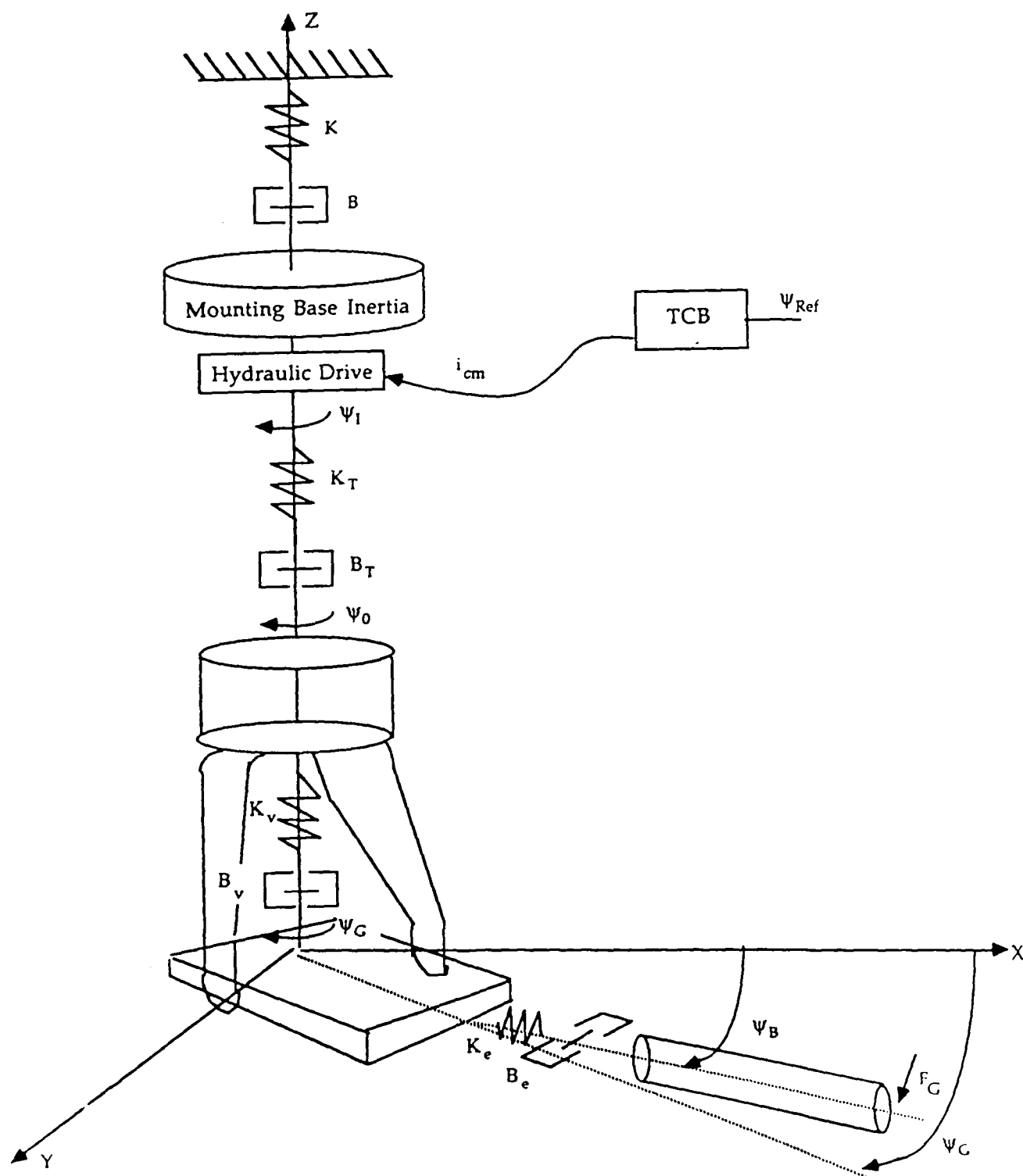


Fig 1. Schematic Diagram of Azimuth Axis System.

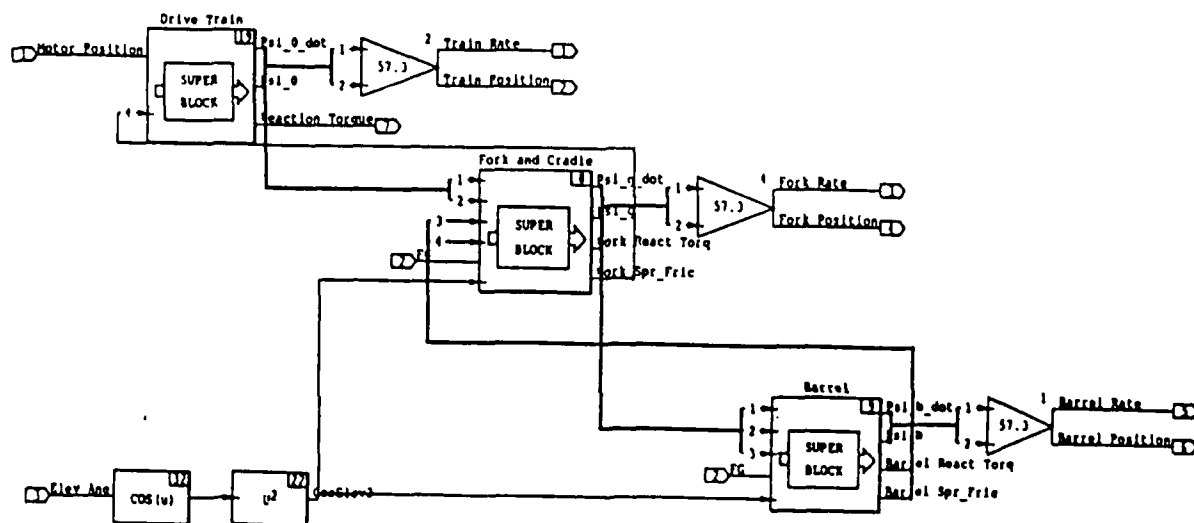
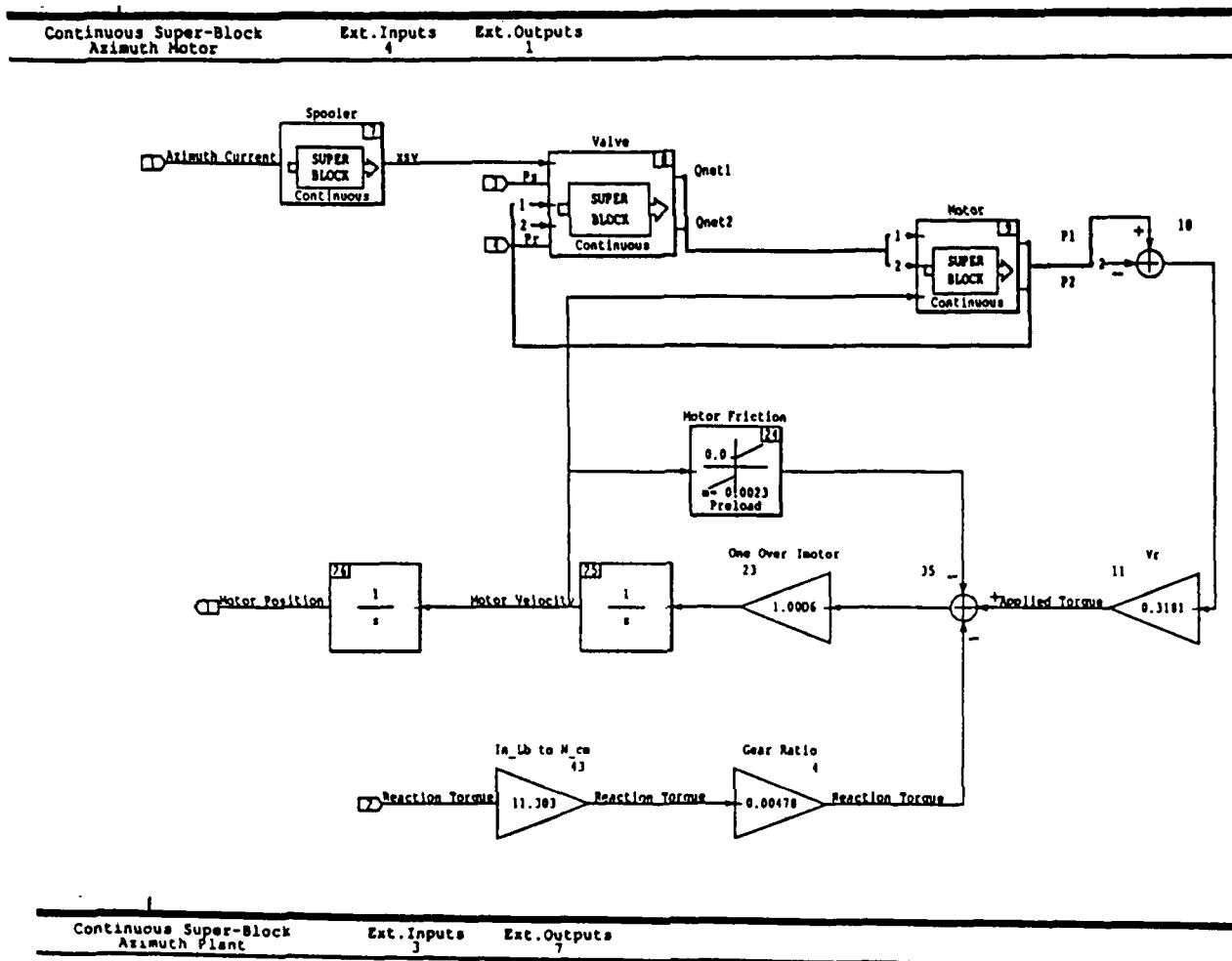


Fig 2. Block Diagram Representation of Azimuth Axis System.

TABLE - I

Eigenvalues, Damping Ratio and Natural Frequencies of Azimuth Axis System

Eigenvalues	Damping Ratio	Natural Frequencies
$-1.713 \times 10^{-3}$		
$-5.375 \pm j52.045$	0.10273	52.322 (rad/sec)
$-20.265 \pm j137.94$	0.14535	139.42 (rad/sec)
$-19.819 \pm j294.8$	0.06707	295.47 (rad/sec)
-945.26		
$-1573.2 \pm j4550.7$	0.32673	4815.0 (rad/sec)
$-122.23 \pm j6397.9$	0.01910	6399.1 (rad/sec)

## VI. DERIVATION OF REDUCED ORDER MODELS

A 12th order linear state variable model of the Turret-Gun System is derived from a nonlinear system by using analyzing systems features of matrix  $x$ . The input and output variables are azimuth current and train rate respectively. A 7th order reduced model is selected on the basis of eigenvalues and singular values. The reduced order models are derived by using balance-truncation, Litz's modal technique and Routh approximation methods. The eigenvalues of the original system and reduced order models are given in Table II. The frequency response plots of original and reduced order models are given in Fig (3). There is an excellent low frequency match between original and reduced order models. Step response comparisons were made between original and reduced order models and are given in Fig (4). It is very hard to see the difference between original and reduced order models.

Table -II      Comparison of Eigenvalues

Original System	Reduced Order Models (7 <sup>th</sup> Order)		
	Balanced - Truncation	Litz's Modal	Routh Method
-1.713 x 10 <sup>-3</sup>	-1.713 x 10 <sup>-3</sup>	-1.713 x 10 <sup>-3</sup>	-1.713 x 10 <sup>-3</sup>
-5.375 ± j52.045	-5.375 ± j52.045	-5.375 ± j52.045	-5.375 ± j52.045
-20.265 ± j137.94	-20.31 ± j138.01	-20.265 ± j137.94	-20.912 ± j138.21
-19.819 ± j294.8	-19.909 ± j294.8	-19.819 ± j294.8	-311.8 ± j541.3
-945.26			
-1573.2 ± j4550.7			
-122.23 ± j6397.9			

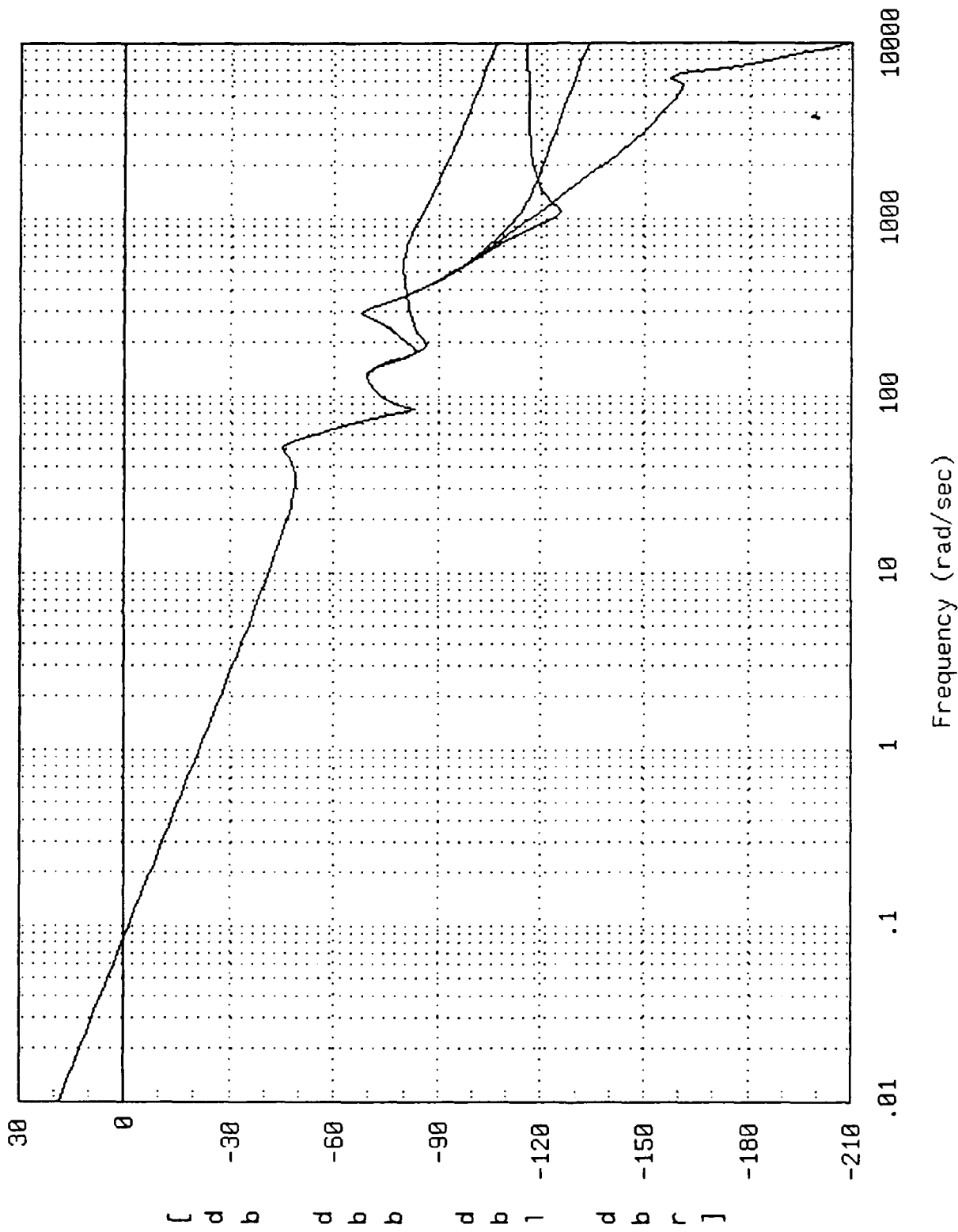


Fig. 3. Frequency Response Plots



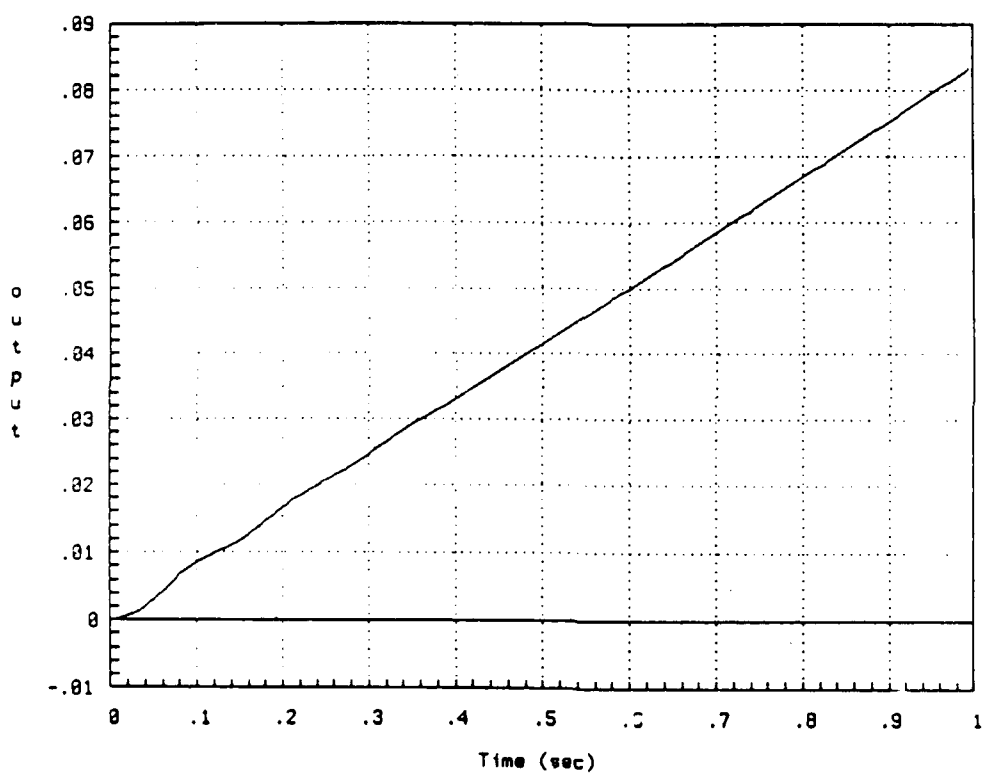


Fig 4. Step Response Plots

## VII ROBUST CONTROLLERS

In recent years, an increased amount of research has been directed toward the design of controllers for the systems whose nominal model is subject to uncertainties. In general the uncertainties in the model arise due to the following causes:

- (1) High frequency dynamics and other characteristics of the plant that are unknown or not well understood. These unmodelled characteristics of the plant also include modes that are ignored when using reduced order models to simplify the controller or the computations involved in design.
- (2) Variations in the plant behavior due to changes in operating conditions. This type of uncertainty is probably best understood and typically occurs in aircraft and other applications where the altitude, pressure, temperature and flight speed all affect the dynamics of the system.
- (3) Errors due to inaccurate or incorrectly calibrated sensors and actuators, and noise introduced by these devices. These uncertainties are generally modelled using frequency domain techniques and involve a stochastic process.

The characterization of the model uncertainties play an important role in the design of LQG/LTR controllers. Hence a brief review of frequency and time domain uncertainties is given below:

(A) Frequency Domain Uncertainties. In the frequency domain, model uncertainties are most often represented by a transfer function matrix, which either multiplies or adds to the transfer function matrix of the nominal plant model. These uncertainties may be assumed to occur either at the input to the plant, or at the output of the plant. Figure 5 shows block diagrams of various frequency domain uncertainty representations. Generally the mathematical model is fairly accurate at low frequencies, so the uncertainties are small. High frequency behavior of real systems is not understood and many times not modeled, so that  $L(s)$  becomes large for high frequencies.

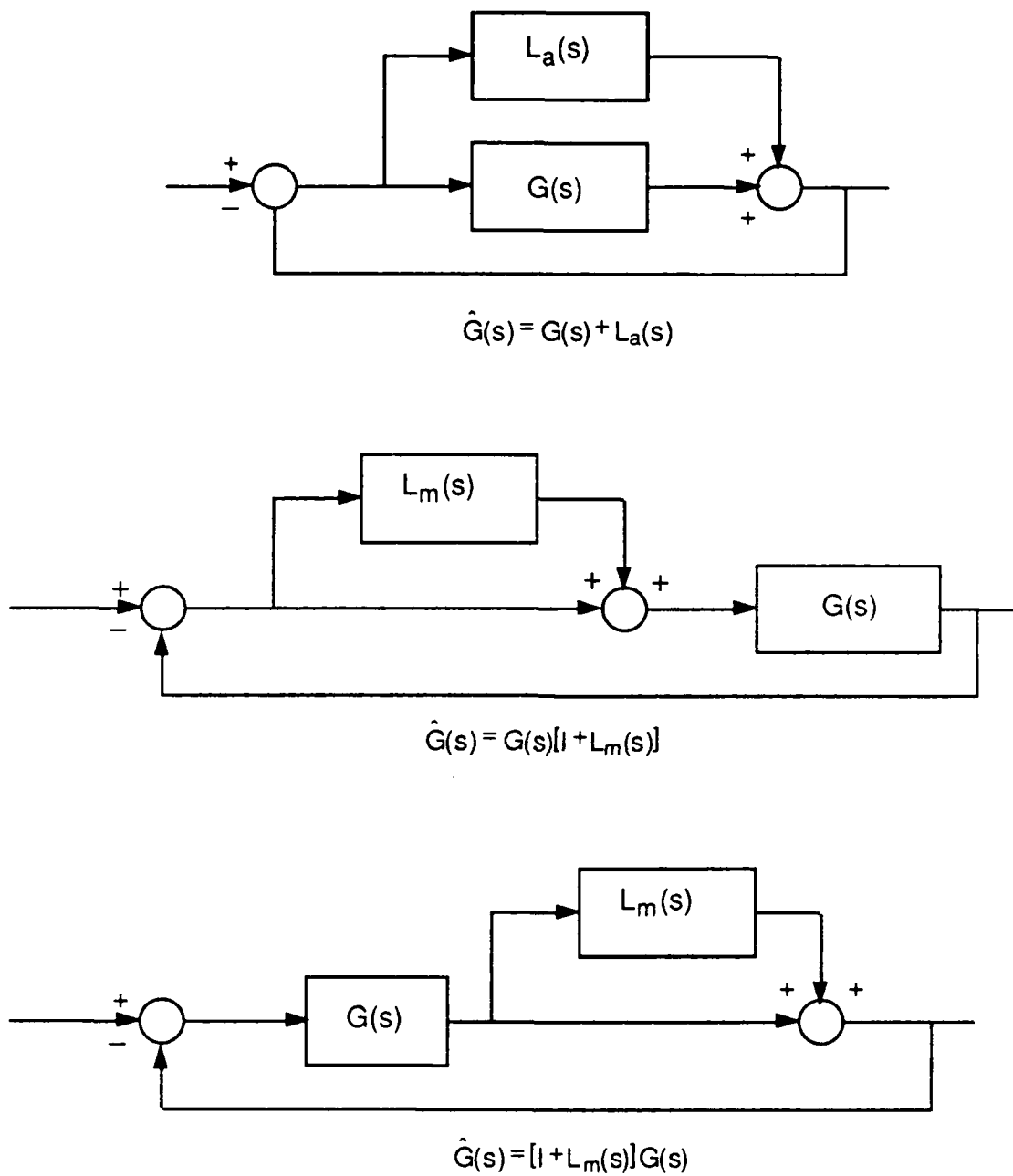


Figure 5. Frequency Domain Representations of Model Uncertainty.  
 a) Additive Uncertainty. b) Input Multiplicative Uncertainty.  
 c) Output Multiplicative Uncertainty.

When discussing the size of a matrix, singular values play an important role. This concept provides a way to quantify the size of a matrix and is defined by

$$\sigma(A) = \sqrt{\lambda(A^H A)} \quad \text{where}$$

$\sigma(A)$  denotes the singular values of  $A$ ,

$\lambda(M)$  denotes the eigenvalues of  $M$ ,

$A^H$  is the complex conjugate transpose of  $A$ ,

$\bar{\sigma}(A)$  is the maximum singular value of  $A$ , and

$\underline{\sigma}(A)$  is the minimum singular value of  $A$ .

It is usually convenient to define a bound on the uncertainties in terms of the maximum singular values.

$$1_a(\omega) > \bar{\sigma}[L_a(s)] \quad \dots(43)$$

$$1_m(\omega) > \bar{\sigma}[L_m(s)] \quad \dots(44)$$

A typical  $1_m(\omega)$  plot is shown in figure 6.

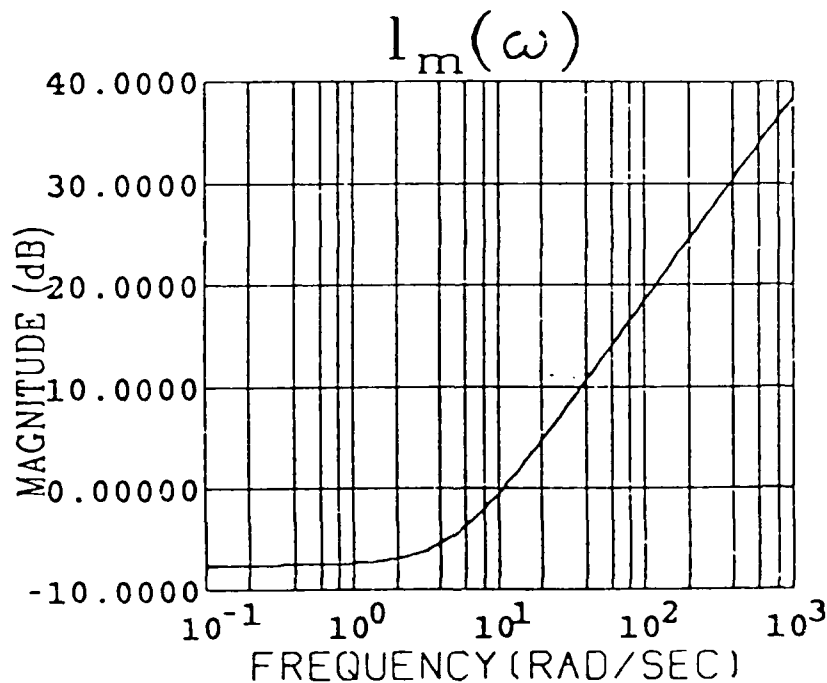


Fig 6 Bound on Frequency Domain Multiplicative Uncertainty.

(B) Time Domain Uncertainties. For time domain analysis a state variable model is most often used for the nominal plant. Uncertainties are therefore represented as changes in the matrices of the state variable model. In most cases, an additive representation is used where an uncertain matrix of appropriate dimension is added to the associated nominal model matrix. The linear state variable model is given by

$$\dot{x} = Ax + Bu \quad \dots(45)$$

$$y = Cx + Du \quad \dots(46)$$

where  $x$  is the state vector of dimension  $n$ ,  $u$  is the input vector with dimension  $m$  and  $y$  is the output vector with dimension  $p$ . For our purposes the uncertainties are assumed to be additive so the general perturbed system is

$$\dot{x} = (A + \Delta A)x + (B + \Delta B)u \quad \dots(47)$$

$$y = (C + \Delta C)x + (D + \Delta D)u \quad \dots(48)$$

### (C) Robustness

A system is said to be robust, with respect to a given class of uncertainties, if for any of those variations in the plant, the overall system behavior remains acceptable. Therefore the designer should be aware of all the variations that can be expected to occur in the real system and be able to describe them so as to insure acceptable behavior in the real system for all conditions. The previous two sections introduced two general methods for describing plant variations or model uncertainties. The way in which acceptable behavior is defined yields two types of robustness.

Stability robustness implies that the system remains stable under the given perturbations, while performance robustness implies that the performance of the system does not deteriorate below acceptable bounds under the given class of perturbations.

### (D) Properties of a Feedback System

The important properties of a feedback system are given below:

## D Properties of a Feedback System

The important properties of a feedback system are given below:  
Consider the feedback system shown in Fig. 7.

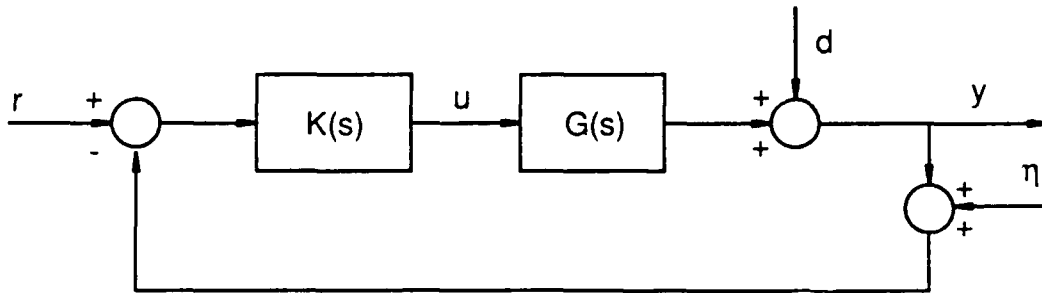


Fig. 7. Typical Feedback System

The output of the closed loop system is given by

$$Y(s) = [I + G(s)K(s)]^{-1}G(s)K(s)[R(s) - \eta(s)] + [I + G(s)K(s)]^{-1}d(s) \quad \dots(49)$$

1. Command Following. The output  $y$  must track the reference input  $r$  so that the transfer function between  $y$  and  $r$  should be approximately equal to the identity matrix.

$$Y(s) = [I + G(s)K(s)]^{-1}G(s)K(s) R(s) \quad \dots(50)$$

If  $G(s)K(s)$  is large, that is if  $\sigma[G(s)K(s)] \gg 1$ , then

$$Y(s) \equiv [G(s)K(s)]^{-1}G(s)K(s)R(s) = R(s) \quad \dots(51)$$

therefore  $y \equiv r$  which is the desired command following characteristic.

2. Disturbance Rejection. The output  $y$  should be rather insensitive to disturbances  $d$ . Consequently the transfer function between  $Y(s)$  and  $D(s)$  should be small.

$$Y(s) = [I + G(s)K(s)]^{-1} D(s) \quad \dots(52)$$

if  $\alpha[G(s)K(s)] \gg 1$ , then  $Y(s) \approx [G(s)K(s)]^{-1}D(s)$  which means  $y$  is insensitive to disturbances when  $G(s)K(s)$  is large.

3. Sensor Noise Rejection. Likewise the transfer function between the output  $y$  and the sensor noise  $\eta$  should be small so that the noise attributed to the sensors has minimal effect on the output.

$$Y(s) = [I + G(s)K(s)]^{-1}G(s)K(s)\eta(s) \quad \dots(53)$$

When  $G(s)K(s)$  is small,  $Y(s) \approx G(s)K(s)\eta(s)$ , so that the noise rejection is achieved. In this case, small  $G(s)K(s)$  is defined as  $\beta[G(s)K(s)] \ll 1$ .

4. Performance Robustness. If there are variations in the plant then the control should be such that the effect on the output is minimal. Let the plant be represented by  $G_n(s) + \Delta G(s)$  where  $G_n$  represents the nominal plant model used in design and  $\Delta G$  represents uncertainties or variations occurring in the real plant. Then the output will have a component due to the nominal system and a component due to the perturbations. This can be represented by

$$Y + \Delta Y = [I + G_n K + \Delta G K]^{-1} [G_n K + \Delta G K] [r - \eta] + [I + G_n K + \Delta G K]^{-1} d \quad \dots(54)$$

where the dependence on  $s$  is not explicitly shown to simplify notation. The change in the output due to the system perturbations is given by

$$\begin{aligned} \Delta Y = & \left\{ [I + G_n K + \Delta G K]^{-1} [G_n K + \Delta G K] - [I + G_n K]^{-1} G_n K \right\} (r - \eta) \\ & + \left\{ [I + G_n K + \Delta G K]^{-1} - [I + G_n K]^{-1} \right\} d \end{aligned} \quad \dots(55)$$

To minimize performance changes due to  $\Delta G(s)$ ,  $\Delta Y$  should be as small as possible. If  $G(s)K(s)$  is large, that is if  $\alpha[G(s)K(s)] \gg 1$  the transfer function becomes

$$\begin{aligned}
\Delta Y &\equiv \left\{ [G_n K + \Delta G K]^{-1} [G_n K + \Delta G K] - [G_n K]^{-1} G_n K \right\} (r - \eta) \\
&\quad + \left\{ [G_n K + \Delta G K]^{-1} - [G_n K]^{-1} \right\} d \\
&\equiv 0(r - \eta) + \left\{ [G_n K + \Delta G K]^{-1} - [G_n K]^{-1} \right\} d \quad \dots(56)
\end{aligned}$$

Therefore  $\Delta Y$  due to  $\Delta G(s)$  is small when  $\underline{\sigma}[G(s)K(s)] \gg 1$ .

Summarizing the above four properties, the gains  $G(s)K(s)$  should be large for command following, disturbance rejection, and performance robustness, but should be small for sensor noise rejection. This is not as contradictory as it may sound, since noise is usually a high frequency phenomenon, while commands, disturbances, and parameter variations are much slower or even constant and thus occur only at low frequencies. Therefore for good performance the loop gains should be large at low frequencies and small at high frequencies. Also for MIMO systems it is generally beneficial to have  $\overline{\sigma}[G(s)K(s)] \equiv \underline{\sigma}[G(s)K(s)]$  so that the performance is similar in all loops. These properties describe desirable feedback system characteristics in the frequency domain. However there is another consideration that puts not just desirable, but necessary constraints on the system transfer function.

5. Stability Robustness. Consider unstructured multiplicative uncertainties at the output of the plant  $\hat{G}(s) = [I + L(s)]G(s)$ , where  $\hat{G}(s)$  represents the actual plant and  $G(s)$  represents the nominal plant model. The system must remain stable for all possible  $L(s)$ . Using the multivariable Nyquist criteria, this requires

$$\overline{\sigma}[(I + GK)^{-1}GK] < \frac{1}{1_m(\omega)} \quad \dots(57)$$

where  $1_m(\omega) \geq \overline{\sigma}L(j\omega)$  [1]. When  $\underline{\sigma}[G(s)K(s)] \gg 1$ ,  $\overline{\sigma}[(I + GK)^{-1}GK] \approx 1$  so that for  $1_m(\omega) < 1$ , the loop gains  $G(s)K(s)$  can be large. When  $1_m(\omega) > 1$ ,  $G(s)K(s)$  must

become small, and when  $1_m(\omega) \gg 1$ ,  $\overline{\sigma}G(s) < \frac{1}{1_m(\omega)}$  so that  $\overline{\sigma}(GK)$  must



decrease rapidly. Thus the crossover frequency of  $1_m(\omega)$  limits the bandwidth of the system by limiting the crossover frequency of  $\bar{\sigma}(GK)$ . This restriction is not just desirable but necessary for stability due to the fact that for some  $L(s)$

where  $\bar{\sigma}L(j\omega) > 1_m(\omega)$  the system will be unstable if  $\bar{\sigma}[(I + GK)^{-1}GK] = \frac{1}{1_m(\omega)}$ .

There is some degree of conservatism associated with this due to the unstructured assumptions inherent in singular value analysis. There may be some  $L(s)$  where  $\bar{\sigma}L(j\omega) > 1_m(\omega)$  but the system remains stable even with

$\bar{\sigma}[(I + GK)^{-1}GK] = \frac{1}{1_m(\omega)}$ . However without specific knowledge of the actual

$L(s)$ ,  $\bar{\sigma}[(I + GK)^{-1}GK]$  must be less than  $1_m(\omega)$  for all  $\omega$  to insure stability.

Then the designer's task is to provide for large loop gains at low frequencies to yield good performance properties, while insuring that the crossover frequency and high frequency rolloff characteristics are adequate to guarantee stability robustness and provide sensor noise rejection. The above analysis has assumed the loop broken at the output. If uncertainties are assumed to occur at the input to the plant, all results are similar except that  $G(s)K(s)$  must be replaced by  $K(s)G(s)$ . For SISO systems these are equivalent, however for MIMO systems they are not.

Among the various methods available for design for robust controllers, the linear quadratic Gaussian with Loop transfer recovery (LQG/LTR) methodology has many advantages. This methodology has been used to design controllers for turret-gun systems. A brief description of LQG/LTR method is given below:

#### (E) LQG/LTR Design Methodology

Doyle and Stein [1] have introduced the LQG/LTR controller methodology and it has become one of the popular controllers for multivariable systems. The LQG/LTR design methodology seeks to define a compensator so that the stability robustness and performance specifications are met to the

extent possible. A well known property of linear quadratic regulators is that they exhibit the following guaranteed stability margins:

$$\frac{1}{2} \leq \text{Gain Margin} \leq \infty \quad \dots(58)$$

$$-60^\circ \leq \text{Phase Margin} \leq 60^\circ \quad \dots(59)$$

However no stability margin guarantees apply when the linear quadratic regulator and Kalman filter are combined into a LQG controller system. This is the motivation behind the loop transfer recovery procedure of the LQG/LTR methodology.

The LQG/LTR design procedure involves two steps. In the first step a target feedback loop is selected which meet the performance specifications. In the second step the tunable parameters of the LQG controller are adjusted so that the performance of the feedback system approximates the performance of the target feedback loop. The LQG/LTR design procedure can be classified into two categories. If the modelling uncertainties is reflected to the output (input) of the plant, a full state Kalman filter (linear quadratic regulator) is designed to meet performance specifications and loop transfer recovery is accomplished with the linear quadratic regulator (Kalman filter). The procedure for the system where the uncertainties are reflected at the output is given below:

#### Full-State Kalman Filter Design

Consider a system represented by

$$\begin{aligned} \dot{x} &= Ax(t) + Bu(t) + \Gamma\xi(t) \\ y &= Cx(t) + \eta(t) \end{aligned} \quad \dots(60)$$

The basic result for the Kalman filter is that the Kalman filter loop transfer matrix

$$T_{KF}(s) = C(sI - A)^{-1}K_f \quad \dots(61)$$

satisfies the following Kalman Equality [15], [16],

$$\begin{aligned} & \left[ I + R_f^{1/2} C (-j\omega I - A)^{-1} K_f R_f^{-1/2} \right]^H \left[ I + R_f^{1/2} C (j\omega I - A)^{-1} K_f R_f^{-1/2} \right] \\ & = I + R_f^{-1/2} C (-j\omega I - A^T)^{-1} Q_f (j\omega I - A)^{-1} C^T R_f^{-1/2} \end{aligned} \quad \dots(62)$$

where  $R_f$  and  $Q_f$  are the control and the states weighting matrices. We note that the above equation is the dual of the LQR. Let us assume

$$R_f = \mu I \quad \dots(63)$$

and

$$Q_f = \Gamma Q_0 \Gamma^T \quad \dots(64)$$

where  $Q_0 = I$  for simplicity. Then equation (62) will be written as

$$\left[ I + T_{KF}(j\omega) \right]^H \left[ I + T_{KF}(j\omega) \right] = I + \frac{1}{\mu} \left[ C(j\omega I - A)^{-1} \Gamma \right] \left[ C(j\omega I - A)^{-1} \Gamma \right]^H \quad \dots(65)$$

The singular value of  $[I + T_{KF}(j\omega)]$  are given by [15]

$$\sigma_i[I + T_{KF}(j\omega)] = \sqrt{1 + \frac{1}{\mu} \sigma_i^2[C(j\omega I - A)^{-1} \Gamma]} \quad \dots(66)$$

This expression governs the performance and stability robustness properties of KF loops [15]. The matrix process noise  $\Gamma$  and the positive scalar  $\mu$  are the tunable parameters. Therefore, the parameters  $\mu$  and  $\Gamma$  are chosen to meet performance, crossover, and robustness properties. It is known that the matrix  $\Gamma$  affects the shape of the TFL singular values plots while  $\mu$  simply raises or lowers the plots.

a. Performance Properties. Good performance, requires high loop gains at low frequencies and satisfies the equation

$$\sigma[T_{KF}(j\omega)] \gg 1 \quad \dots(67)$$

For systems with  $\sigma[T_{KF}(j\omega)] \gg 1$ , the Equation (66) becomes

$$\sigma_i[T_{KF}(j\omega)] \equiv \frac{1}{\sqrt{\mu}} \sigma_i[C(j\omega I - A)^{-1} \Gamma] \quad \dots(68)$$

Thus  $\Gamma$  and  $\mu$  are chosen to meet the low frequency performance requirements. It is important to notice that instead of solving the ARE for the Kalman filter gain  $K_f$  to find  $T_{KF}(s)$  of Equation (61), it is easier to have different choices of  $\Gamma$  and  $\mu$  so Equation (68) can be satisfied. Also,  $\Gamma$  may be chosen to bring  $\underline{\sigma}[T_{KF}(s)]$  and  $\overline{\sigma}[T_{KF}(s)]$  closer together, which typically produces a better design.

b. Crossover Properties. From Equation (66), it is obvious that the KF return difference matrix always exceeds unity, i.e.,

$$\underline{\sigma}[I + T_{KF}(j\omega)] > 1 \quad \forall \omega \quad \dots(69)$$

which implies that

$$\underline{\sigma}[I + T_{KF}^{-1}(j\omega)] > \frac{1}{2} \quad \forall \omega \quad \dots(70)$$

At crossover, it is desirable to bring the minimum and maximum singular values plots of  $T_{KF}$  closer together.

c. Robustness Properties. The relationship,  $\overline{\sigma}[GK(I + GK)^{-1}] \leq \frac{1}{1_m(\omega)}$ , is equivalent to

$$\underline{\sigma}[I + (G(j\omega)K(j\omega))^{-1}] \geq 1_m(\omega) \quad \dots(71)$$

The objective is to approximate the open-loop transfer matrix  $G(j\omega)K(j\omega)$  with  $T_{KF}(j\omega)$ . Hence, Equations (70) and (71) have the same form. Therefore, KF loops are guaranteed to remain stable for all unstructured uncertainties

reflected to the output of the plant which satisfy  $1_m(\omega) < \frac{1}{2}$ . This guarantee will cover the typical low frequency uncertainties, but we have seen that  $1_m(\omega)$  usually grows greater than unity at high frequencies. Thus, it is necessary to

directly manipulate the high frequency behavior of  $T_{KF}(j\omega)$ . this behavior can be derived from known asymptotic properties of the regulator as the scalar  $\mu$  tends to zero [15], [16]. The result needed here is that under minimum phase assumption on  $C(sI-A)^{-1}\Gamma$ , the KF gains  $K_f$  behave asymptotically as

$$\sqrt{\mu}K_f \rightarrow W\Gamma \quad \text{as } \mu \rightarrow 0 \quad \dots(72)$$

where  $W$  is an orthogonal matrix. At high frequencies,  $j\omega$  can be represented

as  $s = \frac{jc}{\sqrt{\mu}}$  as  $\mu \rightarrow 0$  with  $c$  constant. Therefore,

$$\begin{aligned} T_{KF}\left(\frac{jc}{\sqrt{\mu}}\right) &= \sqrt{\mu}C(jcI - \sqrt{\mu}A)^{-1}K_f \\ &\rightarrow \frac{WC\Gamma}{jc} \quad \text{as } \mu \rightarrow 0. \end{aligned} \quad \dots(73)$$

Crossovers occur at  $\sigma_i[T_{KF}(j\omega)] = 1$ , this means that the maximum crossover frequency of the loop should be

$$\omega_{c \max} \leq \frac{\bar{\sigma}[C\Gamma]}{\sqrt{\mu}} \quad \dots(74)$$

This frequency cannot be much beyond the frequency where the output multiplicative uncertainties  $1_m(\omega)=1$ . Therefore, choices of  $\Gamma$  and  $\mu$  that satisfy the performance requirement (68) must all satisfy

$$\omega_{c \max} \leq \omega_1 \quad \dots(75)$$

where  $\omega_1$  is defined as the frequency where  $1_m(\omega_1)=1$ . Hence, the choices of  $\Gamma$  and  $\mu$  to achieve performance objectives via (68) are constrained by the stability robustness requirement via (74).

Loop Transfer Recovery using LQR. After designing the full-state Kalman filter loop to have good performance, crossover, and robustness properties, we need to add a regulator into the system to recover the

guaranteed stability margins. This recovery procedure requires that the plant transfer matrix  $G(s)$  and the target feedback loop  $T_{KF}(s)$  should be square and the plant  $G(s)$  should be minimum phase.

The goal here is to find a procedure to recover guaranteed margins by selecting proper LQR gains. Banda and Ridgely [15] have presented a detailed description of the procedure. The important results are discussed in this section. It is desirable to choose the LQR gains  $K_c$ , so that the loop properties will be the same for the full-state and regulator-based feedback cases. The feedback gain matrix  $K_c$  can be expressed as a function of a scalar parameter  $q$  such that

$$\frac{K_c}{q} \rightarrow WC \quad \text{as } q \rightarrow \infty \quad \dots(76)$$

where  $W$  is any nonsingular matrix. The LQR gains are given by

$$K_c(q) = R_c^{-1} B^T P(q) \quad \dots(77)$$

where  $P(q)$  is the solution of algebraic Riccati equation

$$A^T P(q) + P(q) A - P(q) B R_c^{-1} B^T P(q) + Q_c(q) = 0 \quad \dots(78)$$

and  $Q_c(q)$  is expressed as a function of  $q$ . Now we redefine the LQR state weighting matrices as

$$Q_c = H^T H + q^2 C^T C \quad \dots(79)$$

The term  $q^2 C^T C$  can be thought of as additional fictitious state noise injected into the system through the outputs to the plant. When  $q = 0$  the standard LQR is obtained. However, as  $q$  is made larger the loop properties become closer and closer to that of the TFL. Since the state weighting matrices become increasingly different from the original ones, then a tradeoff between loop recovery and accuracy of the LQR is necessary.

Substituting the weighting Equations (79) into the regulator ARE (78), we get

$$A^T P(q) + P(q)A + H^T H + q^2 C^T C - \frac{1}{\rho} P(q) B B^T P(q) = 0 \quad \dots(80)$$

$$A^T \frac{P(q)}{q^2} + \frac{P(q)}{q^2} A + \frac{H^T H}{q^2} + C^T C - \frac{1}{\rho} q^2 \frac{P(q)}{q^2} B B^T \frac{P(q)}{q^2} = 0 \quad \dots(81)$$

By assuming that  $C(sI-A)^{-1}B$  is minimum phase and the system has as many inputs as many outputs we get,

$$\frac{P(q)}{q^2} \rightarrow 0 \quad \text{as } q \rightarrow \infty \quad \dots(82)$$

As a result when  $q \rightarrow \infty$  we get

$$q^2 \frac{P(q)}{q^2} B R_c^{-1} R_c^{-1} B^T \frac{P(q)}{q^2} \rightarrow C^T C \quad \dots(83)$$

and then

$$\frac{K_c^T(q) R_c K_c(q)}{q} \rightarrow C^T C \quad \text{as } q \rightarrow \infty \quad \dots(84)$$

If we define  $W$  as

$$W = R_c^{-1/2} \quad \dots(85)$$

we will get

$$\frac{K_c(q)}{q} \rightarrow WC \quad q \rightarrow \infty \quad \dots(86)$$

This equation is identical to Equation (76). Hence, choosing the regulator weights as in (79) yields regulator gains, that give same loop properties in the limiting case as  $q \rightarrow \infty$ .

Alternatively the recovery procedure can be thought as a way to approximate the open loop transfer matrix  $G(s)K(s)$  by the TFL transfer matrix  $T_{KF}(s)$ . As  $q^2 \rightarrow \infty$ , we have

$$\begin{aligned}
G(s)K(s) &= C\Phi BK_c[\Phi^{-1} + BK_c + K_f C]^{-1}K_f \\
&\rightarrow C\Phi B[(C\Phi B)^{-1}C\Phi K_f] = C\Phi K_f
\end{aligned}
\quad \dots(87)$$

where  $\Phi = (sI - A)^{-1}$ . This equation shows explicitly that the recovery inverts the plant transfer matrix from the right and the cancellation of the transmission zeros by their inverses. Hence the plant must be minimum phase.

## VIII FREQUENCY SHAPED LINEAR QUADRATIC REGULATOR

In order to place an increased cost on the output of a dynamical system over a specified frequency range, a modification to the standard linear quadratic regulator cost functional is required. The concept of a frequency-shaped linear quadratic regulator (FSLQR) was first introduced by Gupta [2] and has received considerable attention in the literature [3-6]. The frequency shaped weighting elements on states and inputs in the cost functional can be treated as compensation networks similar to those used in classical control.

Consider a linear system represented by

$$\dot{x} = Ax + Bu \quad \dots(88)$$

with performance index

$$J = \frac{1}{2} \int_0^{t_f} \{x^T A x + u^T R u\} dt \quad \dots(89)$$

To understand the concept of frequency shaping it is necessary to write Eq (89) in the frequency domain.

$$J = \frac{1}{2} \int_{-\infty}^{\infty} \{X^*(j\omega) Q X(j\omega) + U^*(j\omega) R U(j\omega)\} d\omega \quad \dots(90)$$

where \* implies complex conjugate. Representation of the cost functional in frequency domain provides a procedure to the use of frequency shaping ideas



in the multivariable techniques. The generalized cost functional can be written as

$$J = \frac{1}{2} \int_{-\infty}^{\infty} \{X^*(j\omega)Q(j\omega)X(j\omega) + U^*(j\omega)R(j\omega)U(j\omega)\} d\omega \quad \dots(91)$$

where  $Q(j\omega)$  and  $R(j\omega)$  are Hermitian matrices at all frequencies. A unique and stable solution that minimizes the cost functional (91) exists when the following conditions are met:

- (i) The pair  $\{A,B\}$  is controllable.
- (ii) The state weighting matrix  $Q(j\omega)$  is symmetric and positive semidefinite.
- (iii) The control input weighting matrix  $R(j\omega)$  is symmetric and positive definite.

The frequency shaped cost functional (92) can also be written as

$$J = \left(\frac{1}{2\pi}\right) \frac{1}{2} \int_0^{\infty} \{X^*(j\omega)Q(\omega^2)X(j\omega) + U^*(j\omega)R(\omega^2)U(j\omega)\} d\omega \quad \dots(92)$$

To develop a control design procedure, let

$$Q(j\omega) = P_1^*(j\omega)P_1(j\omega) \quad \dots(93)$$

$$R(j\omega) = P_2^*(j\omega)P_2(j\omega) \quad \dots(94)$$

Define

$$X_1(j\omega) = P_1(j\omega)X(j\omega) \quad \dots(95)$$

$$U_1(j\omega) = P_2(j\omega)U(j\omega) \quad \dots(96)$$

Then the performance index (92) is represented by

$$J = \left(\frac{1}{2\pi}\right) \frac{1}{2} \int_0^{\infty} \{X_1^*(j\omega)X_1(j\omega) + U_1^*(j\omega)U_1(j\omega)\} d\omega \quad \dots(97)$$

Equation (95) may be expressed in terms of a differential equation or state variable form by assuming the number of zeros in  $P_1(j\omega)$  does not exceed the number of poles. Let the state variable representation of (95) be given by

$$X_1(s) = P_1(s)X(s) \quad \dots(98)$$

$$\dot{z}_1 = A_1 z_1 + B_1 x \quad \dots(99)$$

$$x_1 = C_1 z_1 \quad \dots(100)$$

Similarly Eq (96) in terms of the state variable equation can be expressed as

$$U_1(s) = P_2(s)U(s) \quad \dots(101)$$

$$\dot{z}_2 = A_2 z_2 + B_2 u \quad \dots(102)$$

$$U_1 = C_2 z_2 + D_2 u \quad \dots(103)$$

The augmentation of Eqns (88), (99) and (101) yields

$$\begin{bmatrix} \dot{x} \\ \dot{z}_1 \\ \dot{z}_2 \end{bmatrix} = \begin{bmatrix} A & 0 & 0 \\ B_1 & A_1 & 0 \\ 0 & 0 & A_2 \end{bmatrix} \begin{bmatrix} x \\ z_1 \\ z_2 \end{bmatrix} + \begin{bmatrix} B \\ 0 \\ B_2 \end{bmatrix} u \quad \dots(104)$$

$$\dot{x}_e = A_e x_e + B_e u \quad \dots(105)$$

The time domain version for the frequency shaped cost functional can be expressed as

$$J = \frac{1}{2} \int_0^{t_f} \{x_1^T x_1 + u_1^T u_1\} dt \quad \dots(106)$$

Substitution of Eqns (100), (103) in (106) and simplification yields

$$J = \frac{1}{2} \int_0^{t_f} \{x_e^T Q_e x_e + u^T R_e u + 2x_e^T Q_{xu} u\} dt \quad \dots(107)$$

where

$$Q_e = \begin{bmatrix} 0 & 0 & 0 \\ 0 & C_1^T C_1 & 0 \\ 0 & 0 & C_2^T C_2 \end{bmatrix}; R_e = D_2^T D_2; Q_{xu} = \begin{bmatrix} 0 \\ 0 \\ C_2^T D_2 \end{bmatrix} \quad \dots(108)$$

By using the standard linear quadratic regulator results for system (105), with performance index (107), we obtain

$$u = -K_e x_e = -K_c x - K_1 z_1 - K_2 z_2$$

...(109)

A block diagram representation of closed loop FSLQR system is shown in Fig. 8.

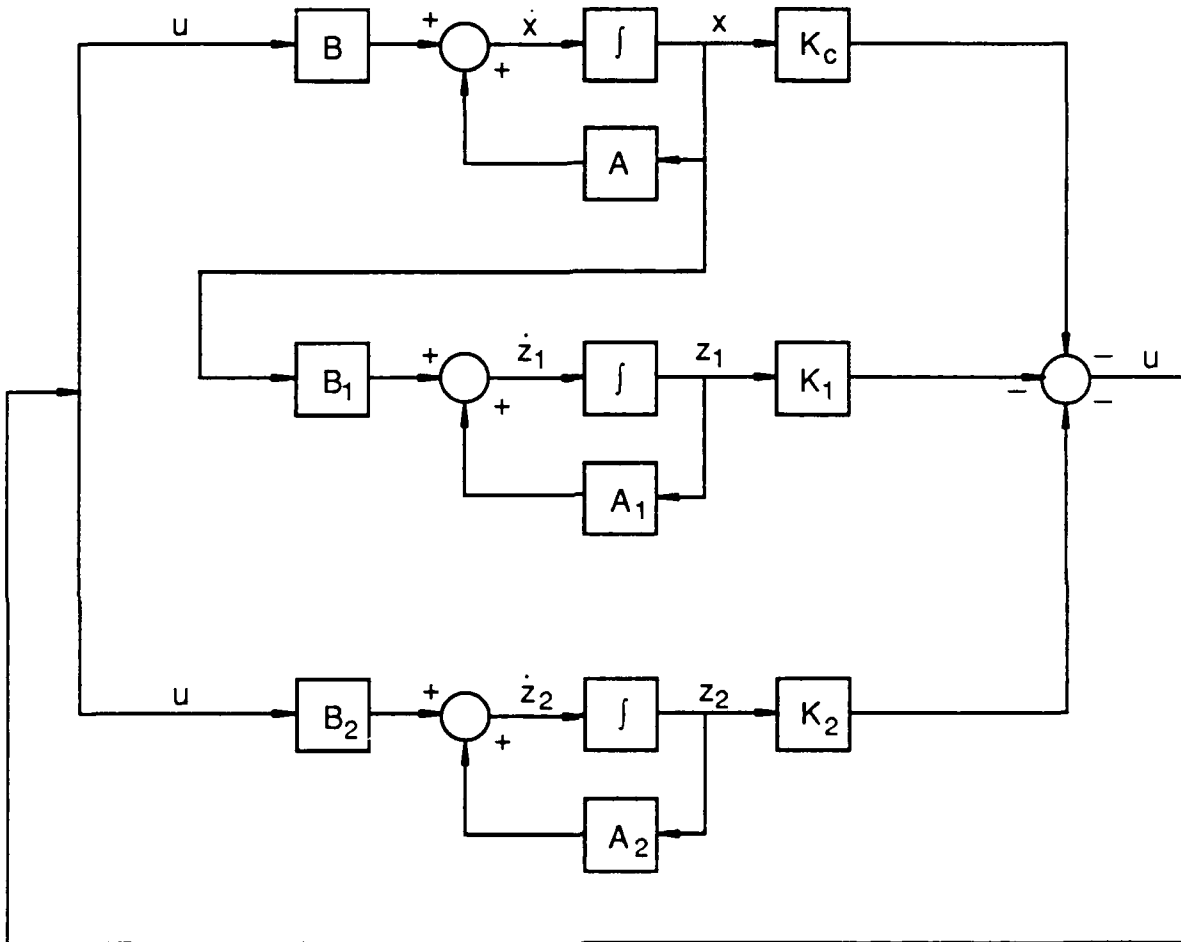


Fig. 8 Block diagram representation of FSLQR closed Loop System.

### (A) Disturbance Attenuation by FSLQR

The effect of disturbances can be reduced by designing a controller so that the sensitivity function of the resultant feedback control system is small over the frequency range where the power spectrum of disturbance is large. Imai et. al [3] have developed a procedure for disturbance attenuation by adjusting the frequency-dependent weighting matrices of the FSLQR method.

Consider a feedback control system shown below:

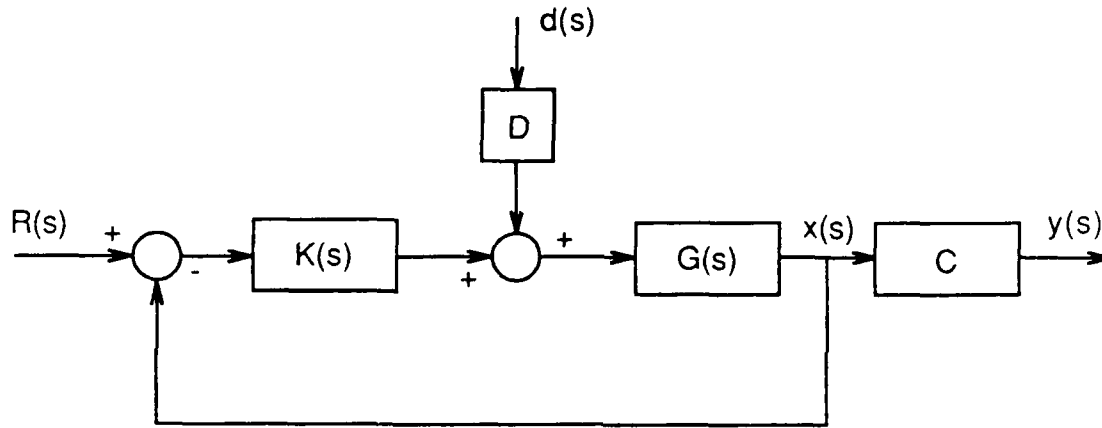


Fig 9. Closed Loop System with Disturbances

$$G(s) = C(sI - A)^{-1}B \quad \dots(110)$$

$$U(s) = -K(s)x(s) \quad \dots(111)$$

The general form of the Kalman equality for the LQR is

$$[I + K_c G(j\omega)]^* R_c [I + K_c G(j\omega)] = R_c + G^*(j\omega) Q_c G(j\omega) \quad \dots(112)$$

The Kalman equality for FSLQR is given by [17]

$$[I + K(j\omega)G(j\omega)]^* R_e [I + K(j\omega)G(j\omega)] = R_e + G^*(j\omega) Q(\omega^2) G(j\omega) \quad \dots(113)$$

Let  $R_e = \rho I$

Then the Kalman equality reduces

$$[I + K(j\omega)G(j\omega)]^* [I + K(j\omega)G(j\omega)] = I + \frac{1}{\rho} [G^*(j\omega)Q(\omega^2)G(j\omega)] \quad \dots(114)$$

The minimum singular value of Eq (114) can be written as

$$\underline{\sigma}^2[I + K(j\omega)G(j\omega)] = I + \frac{1}{\rho} \lambda_{\min}[Q(\omega^2)] \underline{\sigma}^2[G(j\omega)] \quad \dots(115)$$

To minimize the effect of disturbances, it is desirable to have

$$\underline{\sigma}^2[I + K(j\omega)G(j\omega)] = I + \frac{1}{\rho} \lambda_{\min}[Q(\omega^2)] \underline{\sigma}^2[G(j\omega)] \geq \mu(\omega^2) \quad \dots(116)$$

where  $\mu(\omega^2)$  is a low order approximation of the power spectral density.

For a minimum phase system Eq(16) is equivalent to

$$Q(\omega^2) = \rho [G(j\omega)G^*(j\omega)]^{-1} [\mu(\omega^2) - 1] \quad \dots(117)$$

#### (B) Robustness Enhancement of FSLQR Method

The major deficiency of the LQR methodology is the underlying assumption that the model is accurate for all frequencies. In most cases, however, the design model is a low frequency approximation and is not accurate at high frequencies. Anderson and Mingori [4] have developed a FSLQR methodology to enhance the robustness of models with high frequency uncertainty. They showed that stability robustness can be enhanced if a lead filter is used in the diagonal elements of  $R(j\omega)$ . For simplicity, their development is described in this section for SIMO (single-input-multi-output) system. The results can be extended to include the MIMO case.

A SIMO system  $S$  is described by

$$S: \quad \dot{x} = Ax + bu, \quad y = Cx \quad \dots(118)$$

where  $x$  is an  $n \times 1$  state vector,  $u$  is the control input,  $y$  is an  $r \times 1$  output vector and  $\{A, b, C\}$  are of appropriate dimensions. The desired cost functional is of the form

$$J = 1/(2\pi) \int_0^\infty [X^*(j\omega) Q_c X(j\omega) + R(\omega^2) U^2(j\omega)] d\omega \quad \dots(119)$$

where  $Q_c = C^T C$  and

$$R(j\omega) = \frac{j\omega\beta + 1}{j\omega\alpha + 1}, \quad \beta > \alpha > 0 \quad \dots(120)$$

A stable solution is guaranteed if  $Q_c$  is positive semidefinite,  $\{A, b\}$  is stabilizable, and  $\{A, C\}$  is detectable. The state space descriptions of  $Q_c$  and  $R(j\omega)$  are:

$$\dot{z} = 0 \quad \dots(121)$$

$$x_1 = C^T C x \quad \dots(122)$$

$$\dot{z}_2 = -\alpha^{-1} z_2 + \beta \alpha^{-1} u \quad \dots(123)$$

$$u_2 = (\beta^{-1} - \alpha^{-1}) z_2 + \beta \alpha^{-1} u \quad \dots(124)$$

The resulting time domain cost functional is

$$J = \int_0^\infty [x_1^T x_1 + u_2^2] dt \quad \dots(125)$$

In order to make the robustness effect more visible, Anderson and Mingori [4] redefined the input of Eqns (123 and 124) as  $u_2$ . Solving for Eqns (123 and 124) for  $u$ , yields

$$\dot{z}_2 = -\beta^{-1} z_2 + u_2 \quad \dots(126)$$

$$u = (\beta^{-1} - \alpha\beta^{-2}) z_2 + \alpha\beta^{-1} u_2 \quad \dots(127)$$

The redefined state equation for the input filter results in the new cost functional

$$J = \int_0^{\infty} [x_1^T x_1 + u^2] dt \quad \dots(128)$$

Applying the FSLQR procedure results in the following optimal control law

$$u_2 = k_c x + k_2 z_2 \quad \dots(129)$$

Taking the fourier transform of Equation (126), solving for  $Z_2(j\omega)$ , and then substituting into the Fourier transform of Equation (129) yields

$$U_2(j\omega) = \frac{j\omega + \beta^{-1}}{j\omega + \beta^{-1} - k_2} k_c X(j\omega) \quad \dots(130)$$

Solving the original problem of  $U(j\omega)$  results in the controller transfer function  $K(j\omega)$ :

$$U(j\omega) = \frac{j\omega\alpha + 1}{j\omega\beta + 1} U_2(j\omega) = \frac{j\omega\alpha + 1}{j\omega\beta + (1 - \beta k_2)} k_c X(j\omega) = K(j\omega) X(j\omega) \quad \dots(131)$$

Anderson and Mingori [4] derived low frequency inequalities for the frequency-shaped design presented here and also for the conventional LQR problem. These inequalities are:

$$|1 + K(j\omega)G(j\omega)|^2 > \left| \frac{j\omega\beta + 1}{j\omega\beta + (1 - \beta k_2)} \right|^2 \quad (\text{FSLQR}) \quad \dots(132)$$

$$|1 + K_c(j\omega)G(j\omega)|^2 > 1 \quad (\text{LQR}) \quad \dots(133)$$

It was proven in Reference [4] that  $k_2$  is less than zero, then at low frequencies the FSLQR system will loose some robustness due to the frequency shaping of the input when compared to the LQR system. The amount of performance robustness lost due to frequency-shaping is approximately  $(1 - \beta k_2)^{-2}$ . For high frequencies, the following approximations exist

$$|K(j\omega)G(j\omega)| \cong -k_c b \alpha \beta^{-2} \omega^{-1} \quad (\text{FSLQR}) \quad \dots(134)$$

$$|K_c G(j\omega)| \cong b^T P b \omega^{-1} \quad (\text{LQR}) \quad \dots(135)$$

Since  $k_2$  is negative, a third inequality applicable for high frequencies can be defined as follows:

$$|K(j\omega)G(j\omega)| < |K_c G(j\omega)| \quad \dots(136)$$

Inequality (136) states that stability robustness is improved when frequency shaping of the input is employed in the form of a lead filter. In fact, if  $\alpha = 0$ , then the high frequency slope of  $K(j\omega)G(j\omega)$  falls at a rate of -40dB/decade.

### IX FSLQR WITH OUTPUT FEEDBACK METHODOLOGY

The implementation of the frequency shaped linear quadratic regulator (FSLQR) requires the availability of states for feedback. This requirement is met by designing an appropriate state estimator. The use of an estimator increases the order of the controller. The order of the controller may be even greater if integrators are included for command following. To alleviate this problem a FSLQR design methodology using output feedback is presented below. Levine and Athans [18] and Moerder and Calise [19] have developed procedures for determination of the optimal constant feedback controllers for multivariable systems. In the proposed method, the concepts of output feedback and frequency shaping are incorporated in the design of controllers.

The salient features of the proposed methodology are given below:

- (i) Frequency-shaped weighting matrices are considered in the cost functional.
- (ii) The linear quadratic regulator with output feedback design methodology is employed.
- (iii) The proposed methodology may result in lower order controllers compared to LQG/LTR methodology (Dependent on the complexity of  $Q(j\omega)$  and  $R(j\omega)$ ).

A brief review of the linear quadratic regulator with output feedback procedure is given below:



Consider a system represented by

$$\dot{x} = Ax + Bu \quad \dots(137)$$

$$y = Cx \quad \dots(138)$$

with C of full rank and the performance index

$$J = \int_0^{\infty} \{x^T Q x + u^T R u\} dt \quad \dots(139)$$

where  $Q \geq 0$ ,  $R > 0$ . It is desired to minimize J by applying output feedback of the form

$$u = -Ky \quad \dots(140)$$

When this optimal control problem has a solution, the feedback gain matrix is given by

$$K = R^{-1} B^T S P C^T (C P C^T)^{-1} \quad \dots(141)$$

Define  $A^* = A - BKC \quad \dots(142)$

The matrices S and P are the solutions of the following algebraic equations:

$$A^{*T} S + S A^* + Q + C^T K^T R K C = 0 \quad \dots(143)$$

$$A^* P + P A^{*T} + I = 0 \quad \dots(144)$$

A numerical algorithm for solving Eqns (161-166) is given [19]. By combining the standard FSLQR results (Section VIII) with output feedback LQR, we have obtained an FSLQR with output feedback design methodology and is given below:

From Eqns (105) and (107), the FSLQR procedure is to minimize

$$J = \frac{1}{2} \int_0^{t_f} \{x_e^T Q x_e + u^T R_e u^T + 2x_e^T Q_{xu} u\} dt \quad \dots(145)$$

subject to

$$\dot{x}_e = A_e x_e + B_e u \quad \dots(146)$$

$$y = C_e x_e \quad \dots(147)$$

It is desired to minimize J by applying output feedback of the form

$$u = -K_e y \quad \dots(148)$$

The optimization solution for

$$\frac{\partial J}{\partial K_e} = 0 \quad \dots(149)$$

is given by

$$K_e = R_e^{-1} B_e^T S_e P_e C_e^T (C_e P_e C_e^T)^{-1} \quad \dots(150)$$

where

$$A_e^* = A_e - B_e K_e C_e \quad \dots(151)$$

$$S_e A_e^* + A_e^{*T} S_e + Q_e + C_e^T K_e^T R_e K_e C_e = 0 \quad \dots(152)$$

$$A_e^* P_e + P_e A_e^{*T} + I = 0 \quad \dots(153)$$

Moerder and Calise [19] proved that the gain algorithm (Eqns 150-153) converges to a local minimum under the following conditions:

- (i) The pair  $\{C_e, A_e\}$  is detectable
- (ii) The matrix  $R_e$  is positive definite
- (iii) Full row rank for  $C$ .

Mariton and Bertrand [20] have introduced a modification to numerical algorithm [19] for solving Eqns (150-153), by comparing the cost of the  $i^{th}$  iteration  $J(i)$  with optimal cost  $J(opt)$ . This comparison is accomplished by defining an optimality factor

$$V(i) = \frac{J(i) - J(\text{opt})}{J(\text{opt})} \quad \dots(154)$$

where  $J(i) = \text{Tr. } [S(i)]$   
 $J(\text{opt}) =$  The cost associated with full state feedback

#### (A) Performance Robustness Design Guidelines

Performance robustness is a measure of how well a control system tolerates parameter variations, external disturbances, and steady state errors. To achieve good performance robustness, the singular values of the loop transfer function  $K(j\omega)CG(j\omega)$  must be greater than 1 at low frequencies. Also, to achieve integral control (i.e. command following), the slope of the singular value plots must be at least -20dB/decade at low frequencies.

In LQR low frequency design, the following approximation exists

$$\sigma_i[K_c G(j\omega)] \cong 1 / \sqrt{\rho} \sigma_i[HG(j\omega)] \quad \dots(155)$$

where  $Q_c = H^T H$ . A similar low frequency approximation exists for the full state feedback FSLQR. Rewriting the Kalman equality as:

$$[I + \hat{K}(j\omega)G(j\omega)]^* R_e [I + \hat{K}(j\omega)G(j\omega)] = R_e + G^*(j\omega)Q(\omega^2)G(j\omega) \quad \dots(156)$$

where  $\hat{K}(j\omega)$  is the full state feedback version of  $K(j\omega)$  and if  $R_e = \rho I$ , then the Kalman equality reduces to

$$[I + \hat{K}(j\omega)G(j\omega)]^* [I + \hat{K}(j\omega)G(j\omega)] = I + \rho^{-1} G^*(j\omega)Q(\omega^2)G(j\omega) \quad \dots(157)$$

The singular values  $\sigma_i$  of the above equation are:

$$\sigma_i^2[I + \hat{K}(j\omega)G(j\omega)] = \sigma_i[I + \rho^{-1}\{Q(j\omega)G_p(j\omega)\}^* Q(j\omega)G(j\omega)] \quad \dots(158)$$

Since  $\sigma_i[I + \hat{K}(j\omega)G(j\omega)] \gg 1$  at low frequencies, then a good low frequency model of the loop transfer function is

$$\sigma_i[\hat{K}(j\omega)G(j\omega)] \cong 1/\sqrt{\rho} \sigma_i[Q(j\omega)G(j\omega)] \quad \dots(159)$$

Modifying equation (159) to include the output feedback constraint yields the low frequency approximation

$$\sigma_i[K(j\omega)CG(j\omega)] \cong 1/\sqrt{\rho} \sigma_i\{[Q(j\omega)C + H]G(j\omega)\} \quad \dots(160)$$

where  $R(j\omega) = \rho I$ .

#### (B) Loop Shaping Procedure

The loop shaping procedure for this problem is the same as the LQR low frequency design outlined by Doyle and Stein [1]. Briefly, the  $\sigma_{\min}$  and  $\sigma_{\max}$  plots of the loop transfer function given in Equation (160) should be as close together as possible, especially at the crossover. The shape of the plots may be altered by changing  $Q(j\omega)$  and  $H$ . The dc gain of the plot can be adjusted for proper 0 dB crossing by tuning the scalar  $\rho$ . The maximum crossover frequency  $\omega_{c\max}$  should be less than the crossover frequency  $\omega_\ell$  of the uncertainty scalar  $L_m(\omega)$ . The uncertainty scalar represents the maximum multiplicative uncertainty in the plant  $G(j\omega)$ . A list of typical frequency shaped weighting elements for  $Q(r)$  and  $R(s)$  are given in Tables III-IV.

TABLE III  
FREQUENCY-SHAPED WEIGHTING ELEMENTS FOR  $Q(s)$

$Q_{ij}(s)$	Application
$\frac{Q_{ij}}{s}$	integrator for command following and elimination of sensor biases
$Q_{ij} \frac{1 + \tau s}{s}$	proportional-integral control
$Q_{ij} \frac{\tau s}{1 + \tau s}$	"wash-out" filter to eliminate steady-state feedbacks or to approximate the derivative function for use in PID controllers
$Q_{ij} \frac{1 + \tau_1 s}{1 + \tau_2 s}$	provide cross-coupling phase lead to decrease gain scheduling points ( $\tau_1 > \tau_2$ )
$\frac{Q_{ij} \omega_a}{s + \omega_a}$	low pass filter to attenuate high frequency noise
$Q_{ij} \frac{s^2 + \omega_a^2}{s^2 + 2\zeta\omega_a s + \omega_a^2}$	notch filter to eliminate bending mode feedback

TABLE IV  
FREQUENCY-SHAPED WEIGHTING ELEMENTS FOR R(s)

$R_{ij}(s)$	Application
$\rho(1 + s / \omega_0)^n$	for models with high frequency uncertainty ( $n = 1, 2, \dots$ )
$\frac{\rho(1 + s / \omega_0)}{(1 + s / \omega_1)}$	for models with high frequency uncertainty ( $\omega_0 < \omega_1$ )
$\frac{\rho(1 + s^2 / \omega_0^2)}{(1 + 2\zeta s / \omega_0 + s^2 / \omega_0^2)}$	eliminate control response at $\omega_0$

#### X DESIGN OF REDUCED ORDER ROBUST CONTROLLERS

In order to minimize the computational and implementation of LQG/LTR methodology, the reduced order models are used for design of controllers. The reduced order models derived by using balance-truncation, Litz's modal and Routh Approximation methods gave identical frequency responses in the range of 0.01 to 1000 rad/sec. The reduced order model derived by using the balance-truncation method is used to design reduced order LQG/LTR controllers.

Let  $K(s)$  and  $K_r(s)$  represent the transfer functions of LQG/LTR controllers designed using the original 12th order system and 7th order reduced model respectively. (Figs. 10 and 11) The singular value plots of the target feedback loop and open loop transfer functions  $G(s) K(s)$  and  $G(s) K_r(s)$  are shown in Fig (12). The eigenvalues of the closed loop systems full and reduced order controllers are given in Table V. From the eigenvalues of the closed loop system, it is evident that the spillover problem is not present in this system.

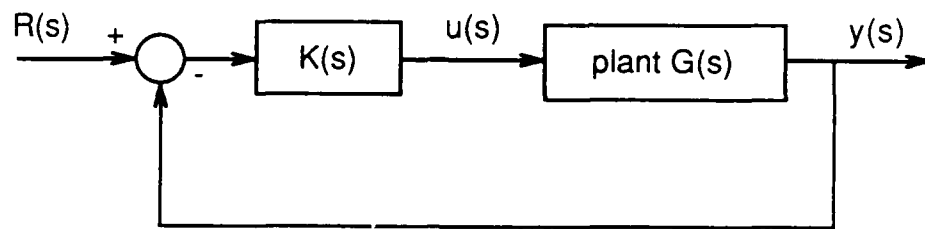


Fig 10. Implementation of Full order Controller.

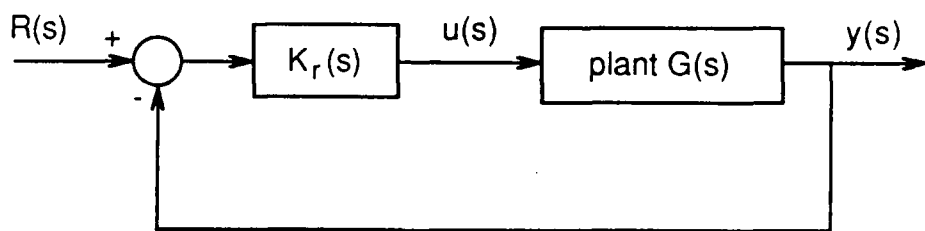


Fig 11. Implementation of Reduced Order Controller.

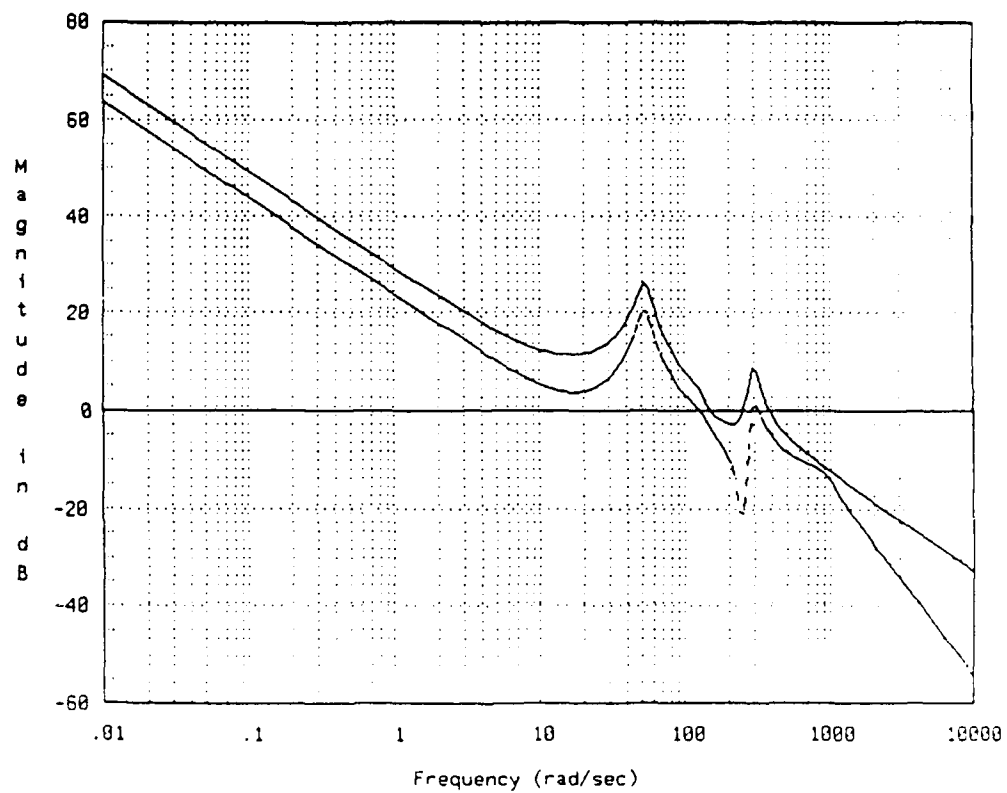


Fig 12. Singular Value Plots



Table V  
Eigenvalue Comparisons of Closed Loop System

12 <sup>th</sup> Order System 12 <sup>th</sup> Order Controller	12 <sup>th</sup> Order System 7 <sup>th</sup> Order Controller
-54.056	-7.6669
-13.177 ± j63.377	-3.4081 ± j82.891
-21.011 ± j138.87	-75.8 ± j57.122
-21.487 ± j295.08	-16.448 ± j140.42
-945.26	-15.721 ± j173.18
-1573.2 ± j4550.7	-62.465 ± j307.78
-122.23 ± j6397.9	-550.88
-0.9278	-320.9 ± j759.85
-2.999 ± j169.96	-1522.2
-217.35 ± j172.77	-1572.9 ± j4550.6
-2258 ± j4380	-122.24 ± j6397.8
-8098.5	
-5984.6 ± j6310.4	
-963.16 ± j9854.0	

The phase and gain margins of the target feedback loop, closed loop systems with original and reduced order controllers are given in Table VI.

TABLE VI

	G <sub>μ</sub>	P <sub>μ</sub>
Target feedback loop	∞	69°
Closed loop system with original controller	22 dB	64°
Closed loop system with reduced order controller	13 dB	61°

### Simulation Results

The parameters of the system matrix are perturbed by 5% and the step responses for full order design and reduced order design are plotted in Fig (13). For the same perturbation, the ramp responses were plotted in Fig (14). Figure (15) contains the step responses with random disturbances at the output.

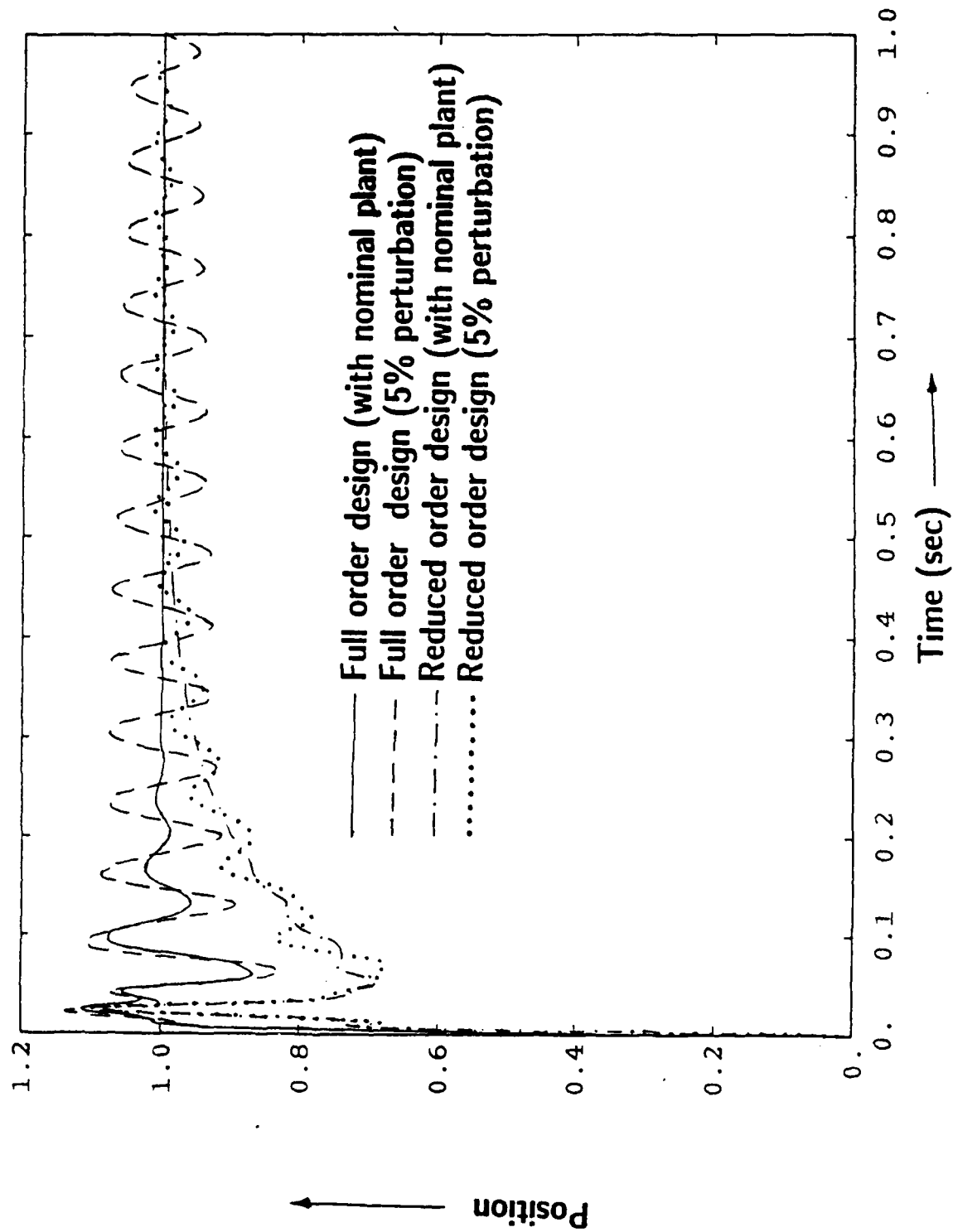


Fig 13. Step Response Comparisons

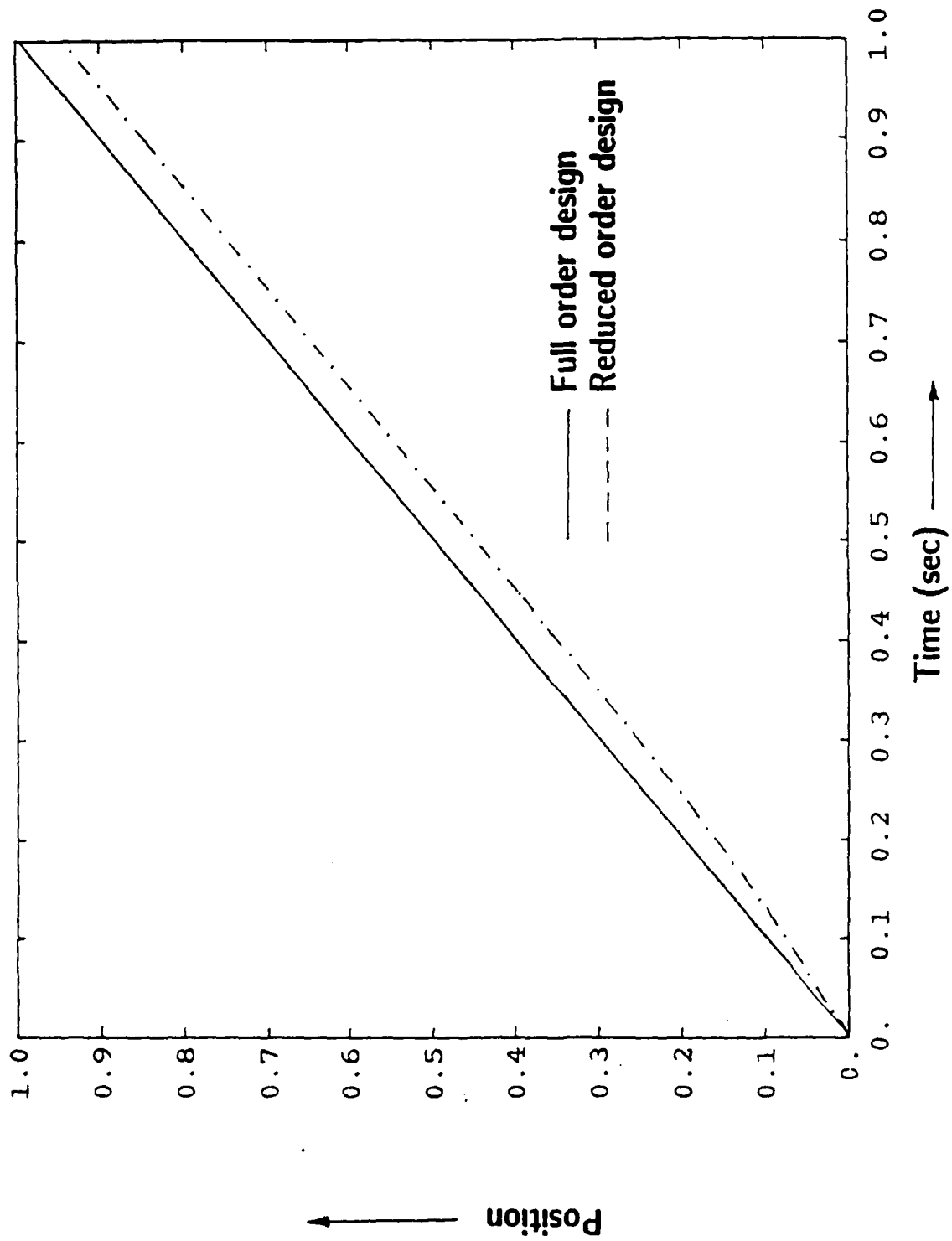


Fig 14. Ramp Response Comparison

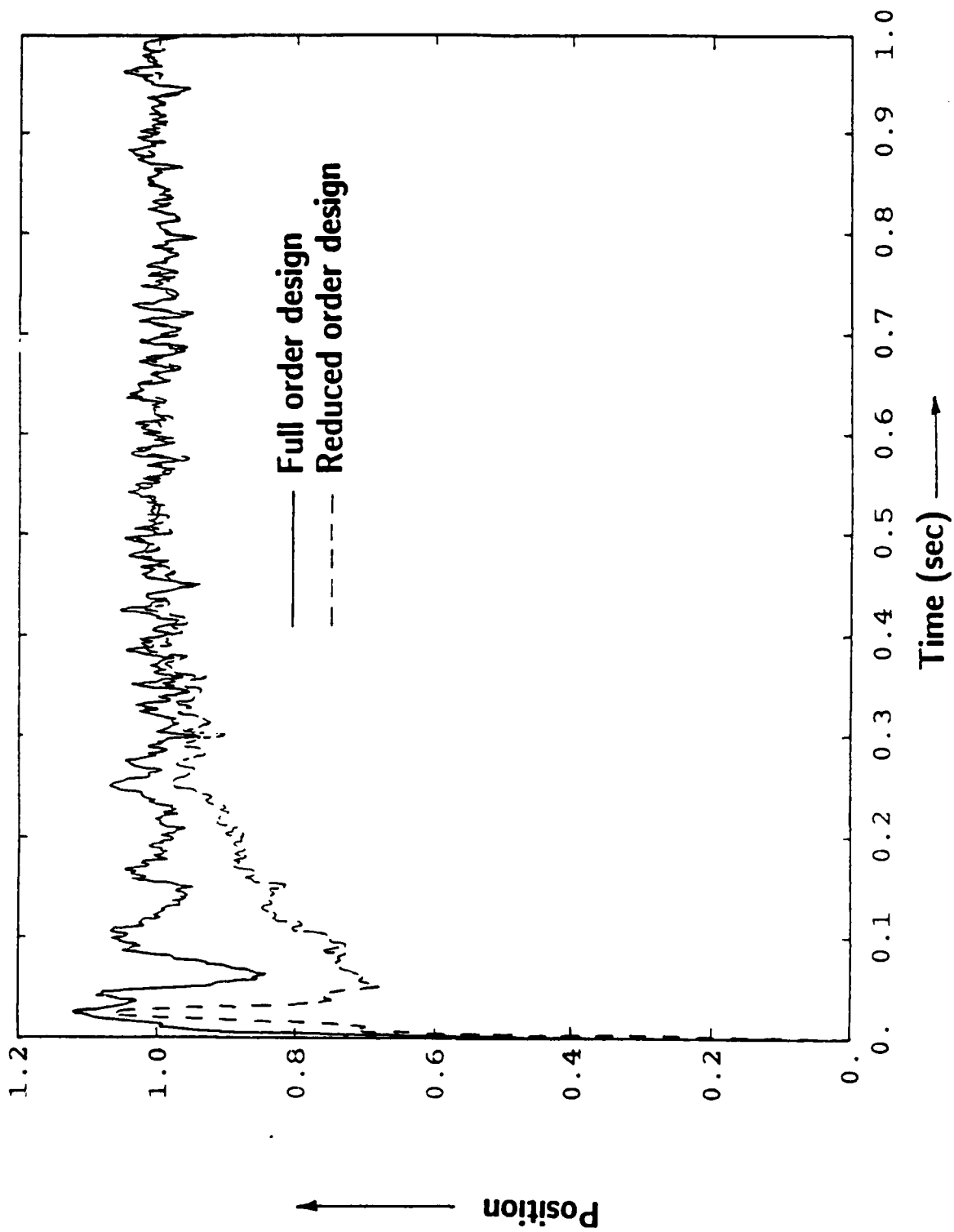


Fig 15. Step Response with Disturbances

## XI CONCLUSIONS

A procedure for the design of robust controllers for a Turret-Gun system mounted on helicopters is presented in this research report. The robust control strategies will guarantee stability and provide satisfactory performance in the presence of model uncertainties. The linear quadratic Gaussian with loop transfer recovery (LQG/LTR) and frequency shaped linear quadratic regulator (FSLQR) with output feedback, design methodologies have been employed to design robust controllers. A description of these design procedures is included in the report. The FSLQR with output feedback is a relatively new approach and is suitable for a turret-gun system.

In order to provide simplicity of implementation and reduction control hardware requirements, a simpler model for the turret-gun system is investigated. Reduced order models are derived by using balance-truncation, Routh approximation and model techniques. The eigenvalues and time responses of reduced order models are compared with the original system. It is very hard to see the difference between step responses of original and reduced order models. There is an excellent low frequency match between original and reduced order models.

The balanced reduced order models are employed to design LQG/LTR controllers. The eigenvalues and stability margins of the reduced order design are compared with the original high order controller. These comparisons and simulation results indicate that the reduced order design gave satisfactory results. The spillover problems are not present in this closed loop system.

The practical implementation of robust controllers on the gun system is an interesting and challenging job. It is recommended that the robust controllers be implemented and compare the response of the open loop and closed loop system for the effects of parameter variations, unmodelled dynamics, sensor and system noises.

## REFERENCES

- [1] J. C. Doyle and G. Stein, "Multivariable Feedback Design: Concepts for a Classical/Modern Synthesis," *IEEE Trans. on Automatic Control*, Vol. AC-26, No. 1, 1981, pp 4-16.
- [2] N. K. Gupta, "Frequency-Shaped Cost Functionals: Extension of the Linear Quadratic Gaussian Design Methods," *Journal. of Guidance, Control and Dynamics*, Vol. 3, No. 6, NW-Dec 1980, pp 529-535.
- [3] H. Imai, N. Abe and M. Kobayakawa, "Disturbance Attenuation by a Frequency-Shaped Linear Quadratic Regulator Method," *Journal. of Guidance, Control and Dynamics*, Vol. 9, No. 4, July-Aug 1986, pp 397-402.
- [4] Anderson, B-D-O. and D. L. Mingori, "Use of Frequency Dependence in Linear Quadratic Control Problems to Frequency-Shape Robustness," *Journal of Guidance, Control and Dynamics*, Vol. 8, No. 3, May-June 1985, pp. 397-401.
- [5] Bossi, J.A., "A Robust Compensator Design by Frequency-Shaped Estimation," *Journal of Guidance, Control and Dynamics*, Vol. 8, No. 4, July-Aug 1985 pp. 541-544.
- [6] Gupta, N.K., M. G. Lyons, J. N. Aubrun, and G. Margulies, "Frequency-Shaping Methods in Large Space Structures Control," Proceedings of AIAA Guidance and Control Conference, AIAA, New York, 1981.
- [7] S. Shah, "Gun/Turret Adaptive Controller for Integrated Air-to-Air Weapon Systems," Report No. 127, Integrated Systems Inc., July 1988
- [8] S. Vittal Rao, M. S. Mattice, N. P. Coleman Jr., "Design of Reduced Order LQG/LTR controllers for Turret-Gun System," Proceedings of American Control Conference, Pittsburgh, June 1989, pp 312-315.

- [9] B. C. Moore, "Principal Component Analysis in Linear System: Controllability, Observability, and Modal Reduction," *IEEE Trans. Automatic Control*, Vol. AC-26, No-1, pp 17-31, Feb 1981.
- [10] L. Litz, "Order Reduction of Linear State-Space Models via Optimal Approximation of the Nondominant Modes," *Proce. of 2nd IFAC Symposium on Large-Scale Systems Toulouse, 1980*, pp 195-202.
- [11] M. F. Hutton and B. Friedland, "Routh Approximation for Reducing Order of Linear Time Invariant Systems," *IEEE Trans. on Automatic Control*, Vol. AC-20 1975, pp 329-337.
- [12] A. S. Rao, S. S. Lamba and S. Vittal Rao, "Routh Approximant Time-Domain Reduced - Order Models for Single - Input Single - Output Systems," *Proce. IEE*, Vol. 125, No. 9, Oct. 1978, pp 1059-1063.
- [13] R. Prakash and S. Vittal Rao, "Model Reduction by Low Frequency Approximation of Internally Balanced Representation," *Proce. of 28th Conference on Decision and Control, Tampa, 1989*.
- [14] D. Bonvin and D. A. Mellichamp, "A Unified Derivation and Critical Review of Modal Approaches to Model Reduction," *Int. J. Control*, 1982, Vol. 35, No. 5, pp 829-848.
- [15] Ridgely, D.B. and S.S. Banda, "Introduction to Robust Multivariable Control," *Air Force Wright Aeronautical Lab, AFWAL-TR-85-3102*, Feb 1986.
- [16] N.A. Lehtomaki, N.R. Sandell and M. Athans, "Robustness Results in Linear-Quadratic Gaussian Based Multivariable Control Designs," *IEEE Trans. on Automatic Control*, Vol. AC-26, No. 1, Feb 1981, pp 75-92.
- [17] V.M. Gonzalez, "Optimal Frequency-Shaped Linear Quadratic Regulator with Output Feedback," *M.S. thesis University of Missouri-Rolla, 1989*.



- [18] Levine, W. S. and M. Athans, "On the Determination of the Optimal Constant Output Feedback Gains for Linear Multivariable Systems," *IEEE Transactions on Automatic Control*, Vol. AC-15, No. 1, pp. 44-48, Feb 1970.
- [19] Moerder, D. D. and A. J. Calise, "Convergence of a Numerical Algorithm for Calculating Optimal Output Feedback Gains," *IEEE Transactions on Automatic Control*, Vol. AC-30, No. 9, pp. 900-903, Sept. 1985.
- [20] Mariton, M. and P. Bertrand, "Output Feedback for a Class of Linear Systems with Stochastic Jump Parameters," *IEEE Transactions on Automatic Control*, Vol. AC-30, No. 9, pp. 898-900, Sept. 1985.

## Distribution List

Commander

Armament Research, Development and Engineering Center

U.S. Army Armament, Munitions and Chemical Command

ATTN: SMCAR-IMI-I (5)

SMCAR-FSF-RC (3)

Picatinny Arsenal, NJ 07806-5000

Commander

U.S. Army Armament, Munitions and Chemical Command

ATTN: AMSMC-GCL (D)

Picatinny Arsenal, NJ 07806-5000

Administrator

Defense Technical Information Center

ATTN: Accessions Division (12)

Cameron Station

Alexandria, VA 22304-6145

Director

U.S. Army Materiel Systems Analysis Activity

ATTN: AMXSY-MP

Aberdeen Proving Ground, MD 21005-5066

Commander

Chemical Research, Development and Engineering Center

U.S. Army Armament, Munitions and Chemical Command

ATTN: SMCCR-MSI

Aberdeen Proving Ground, MD 21010-5423

Commander

Chemical Research, Development and Engineering Center

U.S. Army Armament, Munitions and Chemical Command

ATTN: SMCCR-RSP-A

Aberdeen Proving Ground, MD 21010-5423

Director

Ballistic Research Laboratory

ATTN: AMXBR-OD-ST

Aberdeen Proving Ground, MD 21005-5066

Chief  
Benet Weapons Laboratory, CCAC  
Armament Research, Development and Engineering Center  
U.S. Army Armament, Munitions and Chemical Command  
ATTN: SMCAR-CCB-TL  
Watervliet, NY 12189-5000

Commander  
U.S. Army Armament, Munitions and Chemical Command  
ATTN: SMCAR-ESP-L  
Rock Island, IL 61299-6000

Director  
U.S. Army TRADOC Systems Analysis Activity  
ATTN: ATAA-SL  
White Sands Missile Range, NM 88002